TELOMERASE-DEPENDENT AGEING IN THE ZEBRAFISH BRAIN

Raquel R. Martins[1,2,4], Savandara Besse[3], Pam S. Ellis[1, 2], Naomi Hartopp[4], Nadiyah Mughal[1, 2], Owain Evans[5], Mina HF Wahib[5], Zerkif Yazigan[5], Heather Mortiboys[4], Michael Rera[3] and Catarina M. Henriques[1, 2]

1. Division of Clinical Medicine, Healthy Lifespan Institute and MRC-Arthritis Research UK Centre for Integrated research into Musculoskeletal Ageing, University of Sheffield, Sheffield, UK
2. Bateson Centre, University of Sheffield, Sheffield, S10 2TN, UK.
3. Institut Jacques Monod (UMR7592), Paris, France.
4. Sheffield Institute for Translational Neuroscience (SITraN), University of Sheffield, 385a Glossop Road, Sheffield S10 2HQ, U.K
5. MBChB Medicine Degree, University of Sheffield

Corresponding author: c.m.henriques@sheffield.ac.uk

GRAPHICAL ABSTRACT

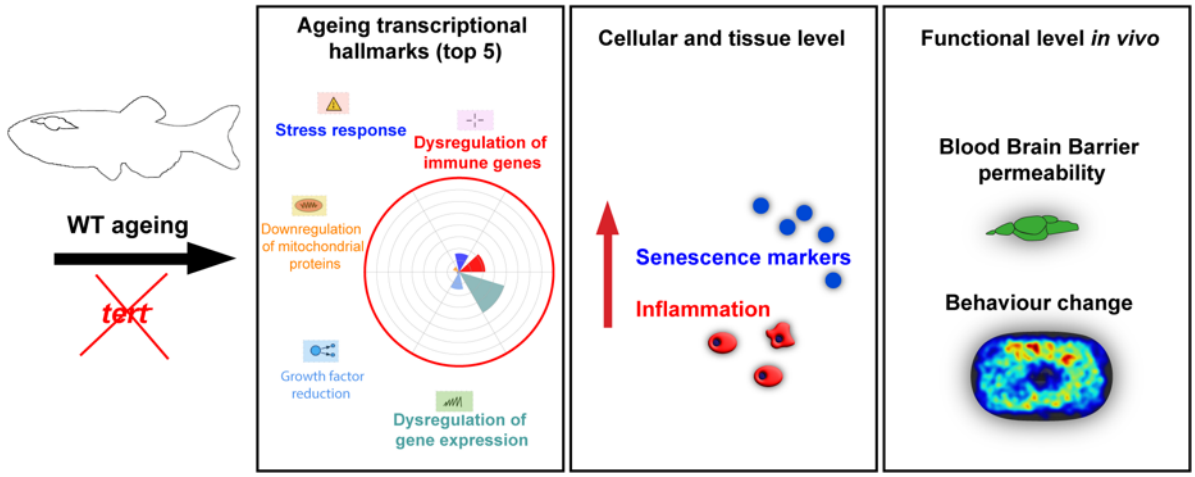

Graphical Abstract: The zebrafish brain displays telomerase-dependent transcriptional hallmarks of ageing which associate with telomerase-dependent accumulation of senescence-associated markers and inflammation in the brain. Importantly, *in vivo*, telomerase deficiency accelerates dysfunction of the blood brain barrier and behavioural change with ageing.

ABSTRACT

Decreased telomerase expression, telomere shortening, senescence-associated markers and inflammation have all been independently observed in the ageing brain and associated with

disease. However, causality between limited telomerase expression and brain senescence and neuro-inflammation in the natural ageing setting is yet to be established. Here, we address these questions using the zebrafish as an ageing model which, akin to humans, displays premature ageing and death in the absence of telomerase and where telomere shortening is a driver of cellular senescence.

Our work shows for the first time that telomerase deficiency (*tert*$^{-/-}$) accelerates key hallmarks of ageing identified in the Wild Type (WT) zebrafish brain at transcriptional, cellular, tissue and functional levels. We show that Tert-dependent transcriptomic changes associated with dysregulation of gene expression, stress response and dysregulation of immune genes are accompanied by accelerated accumulation of senescence-associated markers and inflammation in the aged brain. Importantly, *In vivo*, these changes correlate with increased blood-brain barrier permeability and altered cognitive behaviour. Of note, telomerase-dependent accumulation of senescence-associated markers in the brain occurs not only in the expected proliferative areas but also in non-proliferative ones, where it is unlikely due to telomere-dependent replicative exhaustion, suggesting that non-canonical roles of telomerase may be involved.

Together, our work suggests that telomerase has a protective role in the zebrafish brain against the accumulation of senescence and neuro-inflammation and is required for blood brain barrier integrity.

KEY WORDS: Zebrafish, telomerase, TERT, ageing, brain, inflammation, Blood Brain Barrier (BBB), senescence, behaviour, transcriptomics

ABBREVIATIONS:

AD, Alzheimer's disease

ALS, amyotrophic lateral sclerosis

ANOVA, analysis of variance

ATH, ageing transcriptional hallmarks

56 BBB, blood brain barrier

57 BCA, bicinchoninic acid

58 bp, base pair

59 BSA, bovine serum albumin

60 Ce, cerebellum

61 Cent, centromere

62 CNS, central nervous system

63 DAPI, 4',6-diamidino-2-phenylindole

64 DAVID, database for annotation, visualization, and integrated discovery

65 DDR, DNA damage response

66 DEG, differential expression gene

67 Die, diencephalon

68 dH2O, distilled water

69 DNA, deoxyribonucleic acid

70 Dpf, day post fertilisation

71 dscDNA, double-stranded cDNA

72 EDTA, ethylenediaminetetraacetic acid

73 ENU, N-ethyl-N-nitrosourea

74 FAM, carboxyfluorescein

75 FISH, fluorescence *in situ* hybridisation

76 GEO, gene expression omnibus

77 GOBP, gene ontology biological pathway

78 h, hours

79 HBSS, Hanks buffered solution

80 IF, immunofluorescence

81 IP, intraperitoneal injection

82 IR, irradiation

83 KCN, potassium cyanide

84 KEEG, Kyoto encyclopaedia of genes and genomes

85 KH_2PO_4, potassium dihydrogen phosphate

86 KO, knock-out

87 LCP1, Lplastin

88 LMF, Wolfson light microscopy facility

89 LPS, lipopolysaccharide

90 MgCl2, magnesium chloride

91 Min, minutes

92 MO, medulla oblongata

93 NaCl, sodium chloride

94 NADH, nicotinamide adenine dinucleotide reduced disodium salt

95 NFkβ, nuclear factor kappa β

96 nm, nanometers

97 NO, novel object

98 NPCs, neural progenitor cells

99 NSCs, neural stem cells

100 O.C.T., mounting media

101 OT, optic tectum

102 PBS, phosphate buffered saline

103 PCA, principal component analysis

104 PCNA, proliferating cell nuclear antigen

105 PFA, paraformaldehyde

106 PNA, peptide nucleic acid

107 RIN, RNA integrity number

108 RNA, ribonucleic acid

109 RPM, revolutions per minute

110 RT, room temperature

111 SASP, senescence-associated secretory phenotype

112 sec, seconds

113 SITraN, Sheffield Institute for Translational Neuroscience

114 SSC, saline-sodium citrate

115 TE, Tris-EDTA

116 Tel, telencephalon

117 Telo, telomere

118 Tert, telomerase

119 TERT, telomerase reverse transcriptase

120 TNFα, tumour necrosis factor alpha

121 WT, wild-typeZIRC, Zebrafish international resource center

122 4-MU-chitotrioside , 4–methylumbelliferyl–β-D-N, N', N"-triacetylchitotriose

123 2,6-DCPIP, 2,6-dichlorobenzenone-indophenol sodium salt

124

125 **1 INTRODUCTION**

126 Brain ageing and related neurodegenerative diseases have dramatic consequences on
127 quality of life and medical care costs. Dementia alone, one of the most prevalent
128 manifestations of neurodegenerative disease affects 23 million people only in the UK and it
129 costs around £26 billion a year to the NHS (Collins et al., 2022; Panca et al., 2019; Wittenberg
130 et al., 2019). Understanding the mechanisms underlying brain ageing will target multiple age-

131 associated brain diseases rather than one disease, aiming to ameliorate quality of life in the
132 elderly.
133
134 There are well-known key hallmarks of ageing, which have recently been expanded and
135 consist of genomic instability, telomere attrition, epigenetic alterations, loss of proteostasis,
136 disabled macroautophagy, deregulated nutrient sensing, mitochondrial dysfunction, cellular
137 senescence, stem cell exhaustion, altered intercellular communication, chronic
138 inflammation and dysbiosis (Lemoine, 2021; Lopez-Otin, Blasco, Partridge, Serrano, &
139 Kroemer, 2023). Telomeres are (TTAGGG)n DNA repeats that together with a complex of
140 proteins (known as Shelterin) create a "cap-like" structure at the end of linear chromosomes
141 (de Lange, 2004), preventing the ends of linear chromosomes from being recognised as
142 deleterious DNA double strand breaks (M. G. Ferreira, Miller, & Cooper, 2004). However, in
143 humans, due to time- and cell-specific-limited telomerase expression, telomeres shorten
144 with each cell division, eventually leading to proliferative exhaustion and replicative
145 senescence (Bodnar, 1998; d'Adda di Fagagna et al., 2003). Even though senescence cells do
146 not proliferate, they are metabolically active, releasing several inflammatory factors, tissue
147 remodelling factors and growth factors, known as Senescence Associated Secretory
148 Phenotype (SASP) (Coppe et al., 2010). Consequently, accumulation of senescent cells
149 contributes to impairment of tissue homeostasis and a low level of chronic inflammation.
150 Importantly, there is accumulation of cellular senescence, which can be thought of as a
151 general stress response (Birch & Gil, 2020; Fridlyanskaya, Alekseenko, & Nikolsky, 2015), with
152 ageing in humans (Dimri et al., 1995) and senescence has been linked to several age-
153 associated diseases (Ovadya & Krizhanovsky, 2014; Tuttle, Luesken, Waaijer, & Maier, 2021).
154
155 Restricted telomerase expression and consequent telomere dysfunction function are key
156 hallmarks of natural ageing in humans, underpinning multiple age-related diseases
157 (Blackburn, Epel, & Lin, 2015). As tissues with high cellular turnover present accelerated
158 telomere erosion (Bodnar, 1998; H. W. Lee et al., 1998), it is reasonable to speculate that
159 telomerase functions are likely to primarily affect highly proliferative tissues. Accordingly,
160 premature accumulation of critically short telomeres has been identified in highly
161 proliferative tissues such as the gut, in tert-deficient animal models, including late
162 generation TERT KO mice and zebrafish *tert*$^{-/-}$ mutants (Anchelin et al., 2013; Carneiro et al.,

2016; Henriques, Carneiro, Tenente, Jacinto, & Ferreira, 2013; H. W. Lee et al., 1998). Nevertheless, because senescence has been shown to "spread", in a phenomenon described as paracrine senescence, telomere-dependent genome instability and replicative senescence may lead to non-cell autonomous increase in senescence-associated markers and inflammation (Lex et al., 2020). This means that the role of telomerase and telomeres is not restricted to highly proliferative tissues. To complicate things further, growing evidence suggests that the Tert component of telomerase also has non-canonical activities, independent of its action at telomeres (Goodman & Jain, 2011; Romaniuk et al., 2018; Segal-Bendirdjian & Geli, 2019; Sung, Ali, & Lee, 2014). In the nucleus, these non-canonical functions include transcriptional regulation of genes involved in inflammation, including nuclear factor kappa β (NFkβ) and tumour necrosis factor alpha (TNFα) (Deacon & Knox, 2018; Ghosh et al., 2012; Mattiussi, Tilman, Lenglez, & Decottignies, 2012), as well as genes involved in cell proliferation (Choi et al., 2008; Sarin et al., 2005) and cell survival (Cao, Li, Deb, & Liu, 2002; Rahman, Latonen, & Wiman, 2005). Telomerase can also translocate to the mitochondria, where it has been shown to play a protective role against DNA damage and oxidative stress (Ahmed et al., 2008; Haendeler et al., 2009). In the brain, considered a predominantly post-mitotic tissue, telomerase has been shown to have a protective role against excitotoxicity (Eitan et al., 2012), oxidative stress (Spilsbury, Miwa, Attems, & Saretzki, 2015), and neuronal death (J. Lee et al., 2010), all involved in neurodegenerative diseases. Studies in late-generation telomerase-deficient mice have suggested that limited telomerase expression is associated with premature accumulation of senescence-associated markers in different cell populations including Purkinje neurons, cortical neurons and microglia (De Felice et al., 2014; Jaskelioff et al., 2011; Jurk et al., 2012; Raj et al., 2015). However, it is still unclear whether this is due to telomere length maintenance or non-canonical functions of telomerase (Choi et al., 2008; Sarin et al., 2005).

There are many different stimuli that can cause cellular senescence, including epigenetic alterations, oxidative stress, mitochondrial dysfunction, inactivation of tumour suppressor genes, mechanical or shear stress, pathogens, and activation of oncogenes (Hernandez-Segura, Nehme, & Demaria, 2018; Tripathi, Misra, Tchkonia, & Kirkland, 2021). What causal role telomerase and telomere dysfunction plays in CNS senescence in humans is, however, not clear, even if implicated (Yu et al., 2023). Nevertheless, telomere shortening has been

195 associated with neurodegenerative diseases, including Parkinson's and AD
196 (Papageorgakopoulou, Bania, Lagogianni, Birmpas, & Assimakopoulou, 2024), including via
197 glia activation and pathogenesis (Vellingiri et al., 2023). Of note, a recent study analysing
198 human brain biobank data from over 30,000 patients identified a positive correlation
199 between shorter leukocyte telomere length (used as a proxy for the patient's general
200 telomere length) and neurodegenerative phenotypes (Topiwala et al., 2023). Additionally,
201 cellular senescence-associated markers have been reported in human neuroinflammation
202 and neurodegenerative diseases. In particular, increased levels of DNA damage checkpoints
203 such as p53, p21 and p16, as well as SASP factors have been observed in the spinal cord and
204 brain of patients with amyotrophic lateral sclerosis (ALS) (De Felice et al., 2014) and
205 Alzheimer's disease (AD) (Bhat et al., 2012), respectively. Higher mRNA levels of p16INK4a in
206 the substantia nigra pars compacta (SNpc) were also observed in post-mortem tissue of
207 patients with Parkinson's disease (PD) compared to healthy controls (Chinta et al., 2018) .
208 Moreover, senescence, neuroinflammation and oligomeric tau have been suggested to
209 associated with AD pathology, recently reviewed here (Gaikwad, Senapati, Haque, & Kayed,
210 2024). Hence, the literature shows that despite being a low proliferative tissue, the CNS
211 accumulates senescence or at least senescence-associated markers, and that this may be
212 associated with brain diseases of ageing. However, causality between limited telomerase
213 expression and increased senescence and neuro-inflammation in the natural ageing setting
214 is yet to be established. Nevertheless, mice models where putative senescent cells have been
215 cleared (Bussian et al., 2018) show an improvement of the cognitive decline in aged mice,
216 suggesting that senescence can actively contribute to it. It remains to be determined which
217 cell populations undergo senescence in natural ageing, in the CNS, and what type of
218 senescence this is, i.e., replicative (telomere-dependent) or stress induced senescence.
219 Understanding whether and how telomerase restriction may contribute to ageing-associated
220 brain degenerative phenotypes would help understand the fundamental mechanisms of
221 brain functional decline and potentially contribute to the uncovering of new therapeutic
222 targets to delay or prevent disease.
223
224 The role of telomerase restriction and its consequences in natural ageing may benefit from
225 additional and complementary models, beyond the mouse, where most lab-strains have
226 significant longer telomeres than humans and show little evidence of replicative senescence

227 (Forsyth, Wright, & Shay, 2002; Gomes et al., 2011; Sullivan et al., 2021). The zebrafish may
228 offer such a model since, like humans, they depend on telomerase for health and lifespan
229 (Anchelin et al., 2013; Carneiro et al., 2016; Henriques et al., 2013; Henriques & Ferreira,
230 2012). As it was shown that the zebrafish brain presents low levels of Tert in the adult brain,
231 which tend to decrease with ageing (Sprungala, 2009; Zambusi, Pelin Burhan, Di Giaimo,
232 Schmid, & Ninkovic, 2020), we hypothesised that limited expression of Tert in the aged
233 zebrafish brain contributes to brain degeneration with ageing. To our knowledge, this
234 manuscript represents the first broad characterisation of zebrafish brain ageing in the
235 presence and absence of telomerase (Tert).
236
237 Our data show that the zebrafish brain undergoes Tert-dependent age-associated changes
238 at both transcriptional and functional levels. In specific, our transcriptomic data and
239 enrichment analysis identified dysregulation of gene expression, stress response and
240 dysregulation of immune genes as the top 3 significantly enriched transcriptional hallmarks
241 of old age (Frenk & Houseley, 2018) in WT. Within these differentially expressed genes
242 (DEGs) of old age (WT young *VS* WT old), we identified about 24% which were accelerated in
243 the absence of Tert. When enriched and mapped to the previously described transcriptomic
244 hallmarks of ageing, these Tert-dependent genes of old age identified the same top 3
245 significantly enriched ageing transcriptional hallmarks (ATH) (Frenk & Houseley, 2018) as the
246 overall DEGs of aged WT. Notably, most of the Tert-dependent hallmarks of ageing already
247 significantly accelerated by the age of 9 months in *tert*$^{-/-}$ zebrafish, contrasting to >30 months
248 in WT. At the tissue level, telomerase-dependent stress response and immune dysregulation
249 transcriptional changes with ageing were accompanied by an accelerated accumulation of
250 senescence-associated markers and inflammation. *In vivo*, these changes correlated with
251 increased blood-brain barrier permeability and altered cognitive behaviour. Together, our
252 work suggests that telomerase has a protective role in the zebrafish brain against the
253 accumulation of senescence and neuro-inflammation and is required for blood brain barrier
254 integrity.
255
256
257
258

259 **2 RESULTS**

260 **2.1 Tert-dependent transcriptomic changes of ageing in the zebrafish brain**

261 Tissue-specific transcriptomic analysis over the life course can offer important insights into
262 the downstream molecular mechanisms underpinning age-associated pathologies.
263 Significant research is being dedicated to these approaches in different animal models,
264 including in mice (Schaum et al., 2020; Tabula Muris, 2020; Zhang, Pisco, Darmanis, & Zou,
265 2021). To identify telomerase-dependent and -independent transcriptional signatures of
266 ageing in the zebrafish brain, we performed RNA-Sequencing of whole brain tissue,
267 throughout the lifespan of WT and telomerase-deficient (*tert*$^{-/-}$) fish (**Fig. 1** and
268 supplementary source data files). While *tert*$^{-/-}$ fish have a lifespan of c. 12-20 months, WT fish
269 typically die between c. 36-42 months of age (Carneiro et al., 2016). The data shown here
270 include 4 age-groups of WT (2, 9, 22 and >30 months), corresponding to young, adult, median
271 lifespan and old, respectively. As the *tert*$^{-/-}$ fish have a shorter lifespan compared with their
272 WT siblings, the data include 3 age-groups of telomerase-deficient fish (2, 9, and 22 months),
273 which correspond to young, medium lifespan and old (see Materials & Methods for further
274 explanation of genotypes and ages chosen) (**Fig 1A**). The reads were aligned to the latest
275 zebrafish genome build GRCz11 (Lawson et al., 2020) and resulted in uniquely mapped read
276 percentages ranging from 92.1% to 94.4%, which is considered good quality (Lawson et al.,
277 2020). To analyse the overall impact of the genotype and age on transcriptomic regulation,
278 we performed a Principal Component Analysis (PCA). We observed that the samples cluster
279 mainly *per* age, but within each age group we observe a distinction between genotypes
280 (**Supp Fig 1A**). This provided the first hint of a change in the ageing transcriptomic profile in
281 the *tert*$^{-/-}$. A summary of the number of significant differentially expressed genes (DEGs) over
282 the life course of WT and *tert*$^{-/-}$ is represented in **Supp Fig 1B-D** (for further details see
283 supplementary source data files).

284

285 To identify a broad transcriptomic signature of old age, we compared gene expression
286 changes between young (c.2 months) and old (>30 months) WT (**Fig 1B**). Once these DEGs of
287 old age were identified (for further details see supplementary source data files), we
288 performed Gene Ontology Biological Pathway (GOBP) and Kyoto Encyclopaedia of Genes and
289 Genomes (KEGG) enrichment analysis (**Fig 1B1**) using DAVID software. GOBP analysis of DEGs
290 of old age identified cell cycle, division, chromatin-organisation and chromosome

291 segregation and downregulation of DNA transcription as the top 5 enriched pathways. KEGG
292 analysis mainly identified pathways involved in immune responses (phagosome, infection,
293 PPAR signalling), cell cycle (cell cycle, cellular senescence) and gene regulation (polycomb
294 repressive complex). To contextualise these pathway enrichments within the hallmarks of
295 ageing, we used a previously described strategy (Zane et al., 2023) (see additional details in
296 Materials and Methods Section 9), whereby known GOBP terms are mapped to
297 experimentally identified ageing transcriptomic hallmarks (ATH) (Frenk & Houseley, 2018).
298 ATH mapping identified dysregulation of gene expression, stress response and dysregulation
299 of immune genes as the top 3 significantly enriched transcriptional hallmarks of old age
300 (Frenk & Houseley, 2018) in WT, followed by growth factor reduction, downregulation of
301 mitochondrial proteins and ribosome downregulation(**Fig 1B2**, **Supp Fig 1C** and
302 supplementary data source files). The specific genes associated with each ATH in WT and
303 *tert*$^{-/-}$ over-time are described in **Supp Fig 3** and supplementary data source files.
304
305 To identify how many of the DEGs of old age were Tert-dependent, we compared DEGs in
306 *tert*$^{-/-}$ zebrafish brains over time with WT DEGs of old age. We selected only the ones that
307 changed in *tert*$^{-/-}$, in the same direction as WT, i.e., either up or downregulated. We then
308 compared these with WT DEGs at each timepoint, to ensure they were indeed accelerated
309 in *tert*$^{-/-}$, i.e., changed at younger ages than WT (**Supp Fig 2**). Using this strategy, we identified
310 704 *tert*-dependent DEGs (**Fig 1 B3**), which comprised c.24% of the total DEGs of old age (WT
311 young *VS* WT old). Most GOBP enriched terms of *tert*-dependent DEGs of old age related to
312 pathways involved in gene transcription and neuronal homeostasis. KEGG analysis identified
313 changes in metabolism and immunity (such as insulin and PPAR signalling pathways), actin
314 cytoskeleton and neuronal stem cell function (hedgehog signalling pathway). When these
315 enrichments were mapped to the previously described ATH (**Fig 1 B4**), the *tert*-dependent
316 gene changes of old age identified dysregulation of gene expression, stress response and
317 dysregulation of immune genes as the top 3 significantly enriched transcriptional hallmarks
318 (Frenk & Houseley, 2018), similarly to the overall DEGs of WT old, and to similar extents.
319 These were followed by growth factor reduction, downregulation of mitochondrial proteins
320 and ribosome downregulation. The specific genes associated with each ATH and whether
321 they were up or downregulated are described in **Fig 1 B5 and** supplementary data source
322 files. Notably, most of the *tert*-dependent DEGs of old age, irrespectively of whether

323 enriched and identified as an ageing transcriptomic hallmark, are already changed by the age
324 of 9 months in *tert*$^{-/-}$ zebrafish, contrasting to >30 months in WT (**Supp Fig2**), highlighting a
325 significant acceleration of these hallmarks of ageing in the absence of telomerase (Tert).

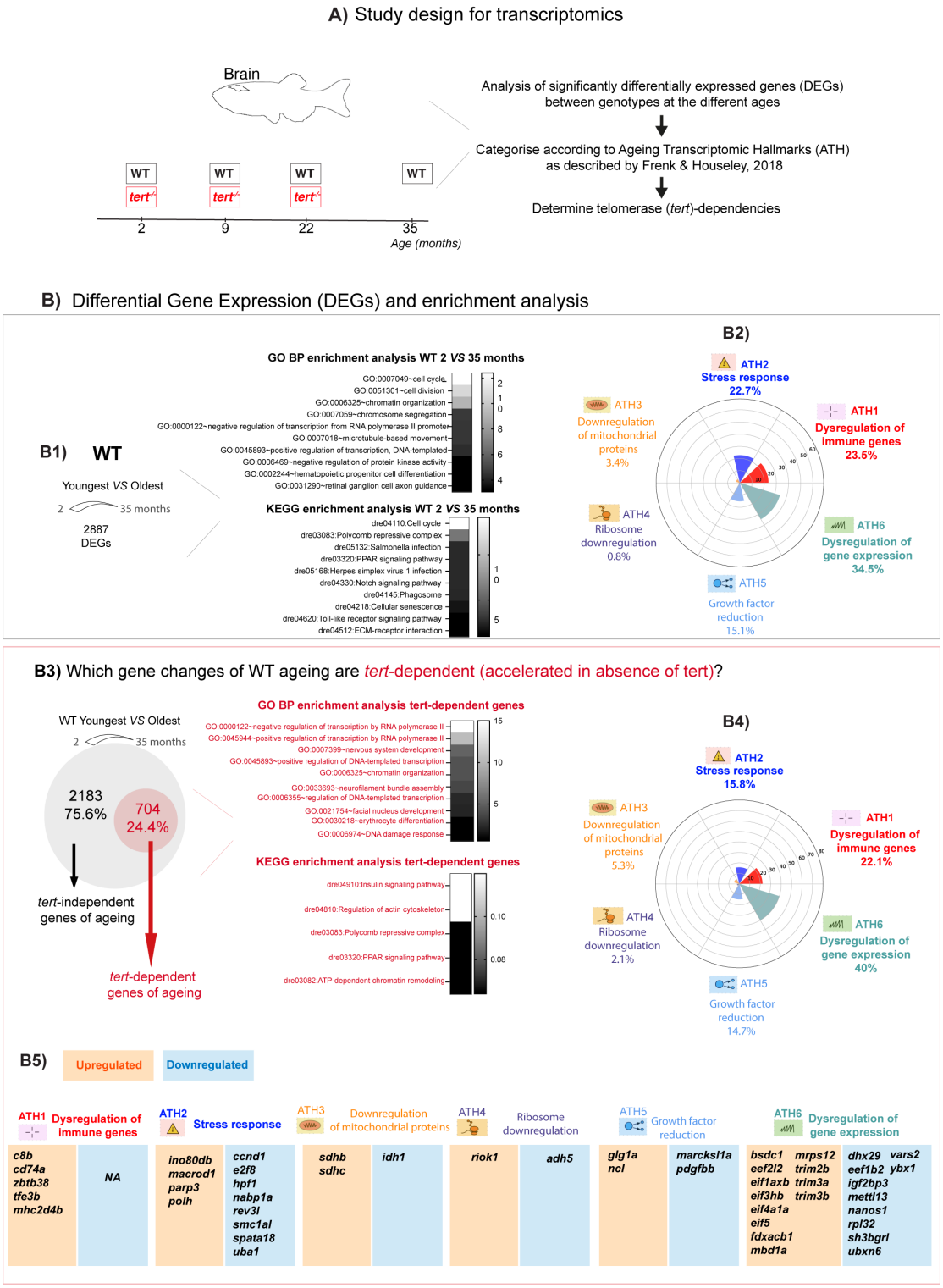

326

327 **Figure 1. Transcriptomic signatures of ageing in the presence and absence of telomerase in the zebrafish**
328 **brain.** (A) Schematic figure of the study design for transcriptomics: RNA from whole brain tissue from young

329 (ca. 2 months), young adult (ca. 9 months), middle aged (ca. 22 months) and old (time of death, >30 months)
330 WT fish, and young (ca. 2 months), middle aged (ca. 9 months) and old (time of death, ca. 22 months) *tert*$^{-/-}$ fish
331 was used for RNA sequencing. N=3 per group. (B1) Differential gene expression (DEGs) analysis using DESeq2
332 identified a total of 2887 DEGs with natural ageing (WT). Heatmaps show the top 10 enriched pathways
333 identified in the GOBP and KEGG databases (analysis performed in DAVID). (B2) The enriched terms and
334 pathways identified to be associated with natural ageing were mapped to the ageing transcriptomic hallmarks
335 (ATH), as previously described (Frenk & Houseley, 2018). (B3) Within the DEGs associated with natural ageing,
336 24.4% (704) were accelerated in the absence of telomerase (*tert*$^{-/-}$). Heatmaps show the top 10 enriched
337 pathways (GOBP and KEGG databases) associated with tert-dependent genes of ageing. (B4) The mapping of
338 the enriched pathways associated with tert-dependent ageing to the ATH showed the same pattern identified
339 in natural ageing, with dysregulation of gene expression, dysregulation of immune system, and stress response
340 being the top 3 significantly changed transcriptional hallmarks of ageing. (B5) Table with the specific genes
341 associated with each ATH.
342

343 **2.2 Tert-dependent stress response with ageing in the zebrafish brain**

344 Given that the top 3 main biological pathways identified by our transcriptomic analysis of old
345 age and telomerase-dependent pathways of ageing included stress response and immune
346 dysfunction, we started by assessing senescence-associated markers in the zebrafish brain,
347 over the life course, in the presence and absence of telomerase (**Fig 2A**). There is not a single
348 marker that can be used on its own to irrefutably identify a senescent cell and markers often
349 described to be associated with senescence in proliferative tissues, such as P16 and P21, are
350 highly expressed in terminally differentiated neurons (Huang, Hickson, Eirin, Kirkland, &
351 Lerman, 2022; Vazquez-Villasenor et al., 2020). This may confound identification of putative
352 senescent cells. Nevertheless, markers such as P16 have previously identified as a good
353 marker for predicting disease progression in Parkinson's Disease (PD) patients (Martin-Ruiz
354 et al., 2020), and with ageing (Idda et al., 2020). Acknowledging these limitations, we
355 performed a broad characterisation of putative cellular senescence as a stress response
356 using four main readouts (Hernandez-Segura et al., 2018): accumulation of Senescence-
357 Associated β Galactosidase (SA-β-Gal) a known biomarker of cellular senescence, at least in
358 most of the cell types tested (Dimri et al., 1995), and often present in different types of
359 senescence (**Fig 2B**); levels of DNA Damage Response (DDR) by γH2AX expression levels (**Fig
360 2C and Supp Fig 4A**); levels of expression of cell cycle kinase inhibitors *p21* and *p16* genes
361 (**Fig 2D**); and proliferation, by Proliferating Cell Nuclear Antigen (PCNA) expression (**Supp Fig
362 4D**).

363 Our initial whole brain SA-β-Gal staining in WT zebrafish brains detected more intense blue
364 staining in WT old (>30 months), when compared to young (c. 5 months) (**Fig 2B and B1**). We
365 then dissected the brains to determine which regions had increased SA-β-Gal staining. At this
366 point, we asked whether SA-β-Gal staining was accelerated in the absence of telomerase, by
367 comparing the staining in WT *versus tert*$^{-/-}$ zebrafish brains. Our results showed a significant
368 increase in SA-β-Gal with ageing in specific regions of the WT zebrafish brain, such as in the
369 midline of the telencephalon, diencephalon, cerebellum and medulla oblongata (**Fig 2B2**).
370 Accumulation of SA-β-Gal in both the diencephalon (quantification shown as a
371 representative example in **Fig 2B3**) and the cerebellum was significantly accelerated in the
372 absence of telomerase (*tert*$^{-/-}$), where, at 5 months, the *tert*$^{-/-}$ brain is already displaying the
373 pattern and levels of SA-β-Gal observed in old WT brains of >30 months of age. Another
374 common marker of senescent cells is the accumulation of DNA damage response (DDR)
375 markers, such as γH2AX foci. Our data show that very few cells accumulate γH2AX foci in the
376 aged brain, in all macroareas tested (never more than 2% of cells). Nevertheless, we did
377 identify a significant increase in the % of γH2AX foci^{+} cells in the diencephalon and
378 cerebellum of old WT, when compared to middle-aged adults, and this was accelerated in
379 *tert*$^{-/-}$ fish (**Fig 2C** and **Supp Fig 4A**). To test whether increase in senescence associated
380 markers correlated with shorter telomeres (i.e. putative replicative senescence), we
381 measured relative telomere length in brain sections of WT fish over time, alongside their *tert*$^{-}$
382 $^{/-}$ counterparts as previously described by us, using a telomeric Peptide Nucleic Acid (PNA)
383 probe alongside a centromeric PNA probe in Fluorescence *in situ* Hybridisation (FISH) (Ellis
384 et al., 2022) (**Fig 2E** and **Supp Fig 4C**). We show that relative telomere length decreases with
385 ageing in WT brains and is significantly shorter in *tert*$^{-/-}$ from an earlier age, as has been
386 shown before for multiple tissues (Carneiro et al., 2016). However, as expected, relative
387 telomere length in the brain is significantly longer than in the highly proliferative gut
388 epithelia of the same individuals, both in WT and *tert*$^{-/-}$, at all ages tested. Despite observing
389 telomere shortening in the brain, we did not detect significant changes in cell proliferation,
390 as assessed by PCNA expression, in any of the areas tested, including in the known
391 proliferative niches present in parts of the diencephalon and midline of the telencephalon
392 (**Supp Fig 4B**). Proliferation levels, however, are very low to start with, and we never
393 detected more than 6% of cells proliferating (**Supp Fig 4D**)**.** Increased levels of p16 and *p21*
394 are usually observed in senescent cells, depending on the stimuli and cell type (Dulic, Beney,

395 Frebourg, Drullinger, & Stein, 2000). We therefore tested whether increased levels of these
396 two cyclin inhibitors correlate with increased levels of SA-β-Gal in different brain regions.
397 Levels of *p16* and *p21* were assessed by RNA *in-situ* hybridisation. We detected increased
398 levels of *p16*, but not *p21*, in the proliferative grey area of the optic tectum and in some
399 regions of the diencephalon of old WT fish, where SA-β-Gal is also observed. Increased SA-
400 β-Gal and *p16* expression was observed at an earlier age, in *tert*$^{-/-}$ fish (**Fig 2D**).

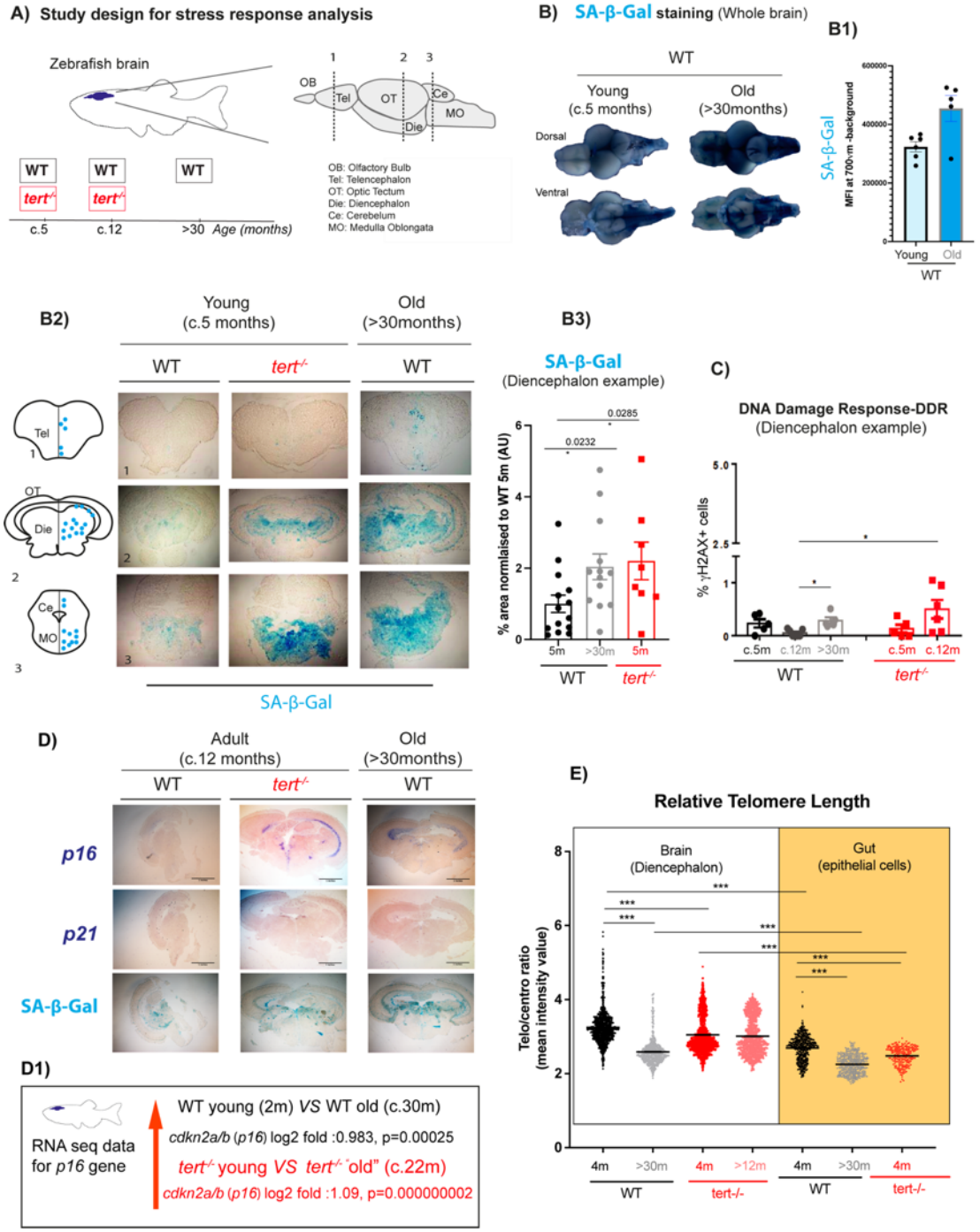

401 **Figure 2. Telomerase-dependent stress response in the zebrafish brain with ageing.** (A) Schematic figure of
402 the study design for stress response: brain tissue collected from young (ca. 5 months), middle aged (ca. 12

403 months) and old (time of death, >30 months) WT fish, and young (ca. 5 months) and old (time of death, ca. 12
404 months) *tert*$^{-/-}$ fish were used to assess stress response through SA-β-Gal staining (in whole brain and coronal
405 cryosections of telencephalon, optic tectum and rombencephalon), telomere length and DNA damage (in
406 longitudinal paraffin sections), and metabolomics (in whole brain tissue). (B) Representative images of SA-B-
407 Gal staining in the whole WT zebrafish brain and (B1) respective quantifications show an increased expression
408 of SA- β -Gal in old WT brains compared to young ones. N=5-6 per group. (B2) Representative images of SA-B-
409 Gal staining in coronal cryosections of WT and *tert*$^{-/-}$ zebrafish show that there is an increased expression of SA-
410 B-Gal in old WT zebrafish and that this is anticipated in young *tert*$^{-/-}$ (ca. 5 months), particularly in the
411 diencephalon for which (B3) quantifications are shown. N=8-14 per group. (C) DNA damage response assessed
412 by γH2AX staining in longitudinal paraffin sections of zebrafish brain show increased DNA damage from 12 to
413 >30 months of age in WT fish, and this increase is anticipated in the absence of telomerase at 12 months of
414 age. N=3-7 per group. (D) Representative images from in-situ hybridisation in coronal cryosections show an
415 increased expression of *p16* but not *p21* in old WT zebrafish optic tectum and diencephalon, in areas where
416 SA- β -Gal expression is observed. This increase in *p16* expression is already significant at 12 months of age in
417 *tert*$^{-/-}$. (E)Telomere/centromere ratio assessed by telo-FISH in longitudinal paraffin sections of zebrafish brain
418 (white) and gut (yellow) show that telomere length decreases with ageing in WT fish and that this is anticipated
419 in young *tert*$^{-/-}$ fish (ca. 5 months). N=4-5 per group. (B1, B3, C) Each dot represents one animal. (E) Each dot
420 represents one cell. Error bars: SEM. * $p<0.05$; ** $p<0.01$; *** $p<0.001$. Abbreviations: OB, olfactive bulb; Tel,
421 telencephalon; Die, diencephalon; OT, optic tectum; Ce, cerebellum; MO, medulla oblongata.
422
423 Different types of senescence stimuli have been identified to express different SASP factors
424 and an attempt has been made to collate the variety of SASP factors assembled by proteomic
425 analysis of conditioned media from different types of *in vitro* senescence (Basisty et al., 2020),
426 some of which can be found in http://www.saspatlas.com/. Additionally, the same work
427 identified 3 key secreted proteins in common to some DDR and DDR-independent types of
428 senescence, namely CXCL1, MMP1 and STC1. Moreover, GDF15, STC1 and SERPINs were
429 identified as SASP-associated factors in aged human plasma (Basisty et al., 2020). Our RNA
430 sequencing data identified 13 putative SASP genes upregulated in aged WT brains, using
431 SASPatlas.com (**Supp. Fig 5**), namely *arpc1b, b2m, ccdc88b, dcn, fhod1, fkbp3, flnb, ifi35,*
432 *itga5, lmna, myo9b, naga, pfn1, psme1 and 2, rbp4, scin and thy1*. Of these, 5 were *Tert*-
433 dependent, namely *arpc1b, fhod1, psme1* and *2 and rbp4*. Interestingly, most of the SASP
434 molecules up-regulated (8 out of 13) in WT aged brains were also upregulated in oncogene
435 induced senescence of fibroblasts, whereas the genotoxic stress SASP in the same cells had
436 less in common with WT aged brains, according to saspatlas.com (**Supp Fig 5**). We therefore
437 searched for these genes in our transcriptomic data and found related molecules upregulated

438 in aged WT zebrafish brains, namely *cxcl12a*, *cxcl32b.1* and *cxcl18b* (zebrafish *cxcl1 per se* has
439 not yet been described); *mmp13b*, *stc2a* and serpina10a, *serpinb1l3* and *serpinb1l1*. Of these,
440 *mmp13b* upregulation was significantly accelerated in *tert*$^{-/-}$ fish, where upregulation is
441 already significant at the age of 2 months, contrasting to >30 months in WT. Additionally,
442 mmp13 is 5 times more upregulated in *tert*$^{-/-}$ at 2 months than WT at >30 months, with log2
443 expression of 5.3 *versus* 1.2, respectively. Expression of this putative SASP gene is not only
444 accelerated but also exacerbated in the absence of Tert (supplementary source data).
445
446 Together, these data show a telomerase-dependent accumulation of cellular senescence-
447 associated markers with ageing in the zebrafish brain (increased SA-β-Gal, DNA damage
448 response, and *p16* expression, and up-regulation of some putative SASP factors), suggesting
449 that Tert has a protective effect against accumulation of senescence in the brain.
450 Interestingly, accumulation of senescence-associated markers was detected in both
451 proliferative and non-proliferative regions of the brain (**Supp Fig 4B**). This could suggest that
452 there are other types of telomerase-dependent senescence accumulating with ageing in
453 addition to classic replicative senescence. One hypothesis is that non-canonical, i.e.
454 telomere-length independent functions of telomerase may also have a protective role in the
455 brain (Segal-Bendirdjian & Geli, 2019).
456
457 **2.3 Tert-dependent inflammation with ageing in the zebrafish brain**
458 Within its non-canonical functions, the Tert component of telomerase (i.e telomerase
459 reverse transcriptase) has been reported to play a role in transcriptional regulation of
460 inflammatory-associated genes (Choi et al., 2008; Ghosh et al., 2012). Moreover, telomere
461 dysfunction has been shown to contribute to a dysfunctional inflammatory environment in
462 the zebrafish model (Lex et al., 2020). Accordingly, our RNA sequencing data identifies
463 immune dysregulation as one of the top 3 telomerase-dependent transcriptional hallmarks
464 of ageing and we wanted to investigate this further at tissue level. We started by assessing
465 overall levels of inflammation in the zebrafish brain, in young and old animals, in the
466 presence and absence of telomerase. Because there is no agreed specific microglia marker
467 in zebrafish, we combined the tg(*mpeg*1.1-mCherry-caax) transgenic zebrafish line (Ellett,
468 Pase, Hayman, Andrianopoulos, & Lieschke, 2011), which has been shown to identify
469 macrophages and microglia in the brain (Oosterhof et al., 2017), with a well-described pan-

470 immune cell marker (L-plastin or LCP-1) (Cvejic et al., 2008; Mathias et al., 2010; Redd, Kelly,
471 Dunn, Way, & Martin, 2006; Van Houcke et al., 2017) and use immunofluorescence (IF) to
472 quantify immune cell populations in the brain (Martins, Ellis, MacDonald, Richardson, &
473 Henriques, 2019) as a readout for inflammation. Using these two markers allowed us to
474 identify macrophages/microglia as L-plastin^{+}*mpeg*$^{+}$ cells, and distinguish them from any
475 other immune cells, which would be L-plastin^{+}*mpeg*$^{-}$ (**Fig 3A).** Our data show that there is an
476 increased number of plastin^{+}*mpeg*$^{+}$ cells (**Fig 3A1**) but not of L-plastin^{+}*mpeg*$^{-}$ cells (**Fig 3A2**)
477 with ageing, in most of the zebrafish brain (WT 5 months *VS* WT 30 months) (**Supp Fig 6**),
478 suggesting a macrophage/microglia specific increase. The macrophage/microglia increase in
479 the brain was accelerated in the absence of telomerase already at the early age of 5 months
480 (WT 5 months *VS tert*$^{-/-}$ 5 months), suggesting that neuroinflammation is as a telomerase-
481 dependent ageing phenotype (**Fig 3A1**).
482
483 To understand whether macrophage/microglia increase with ageing was associated with
484 immune activation, we used a chitotriosidase activity assay. Chitotriosidase is an enzyme
485 expressed by activated macrophages and other phagocytic cells and can therefore be used
486 as a biomarker of microglia/macrophage activation, including in zebrafish (Keatinge et al.,
487 2015). Our data show that there are increased levels of chitotriosidase in the naturally aged
488 brain (WT 4-6 *VS* 14-16 *VS* 30 months) and that this is accelerated in the absence of
489 telomerase from the age of 14-16 months, suggesting that neuronal immune activation is a
490 telomerase-dependent phenotype of ageing (**Fig. 3B**).
491
492 Accumulation of cellular senescence is thought to contribute to chronic inflammation in
493 ageing, often termed "inflammageing" (Deleidi, Jäggle, & Rubino, 2015; Franceschi &
494 Campisi, 2014; M, Selman;, Lene, & Bellantuono, 2016). On one hand, in some contexts,
495 immune cells have been shown to be recruited to sites of cellular senescence (Demaria et
496 al., 2014; Krizhanovsky et al., 2008). On the other hand, senescent cells have been shown to
497 release pro-inflammatory factors (part of SASP), which can contribute to paracrine
498 senescence (Acosta et al., 2013) as well as to tissue inflammation (Franceschi & Campisi,
499 2014). We therefore set out to determine how the increased levels of senescence-associated
500 markers we detected in the zebrafish brain correlated with immune cell numbers. To do this,
501 we performed IF staining with the pan-immune cell marker L-plastin on SA-β-Gal-stained

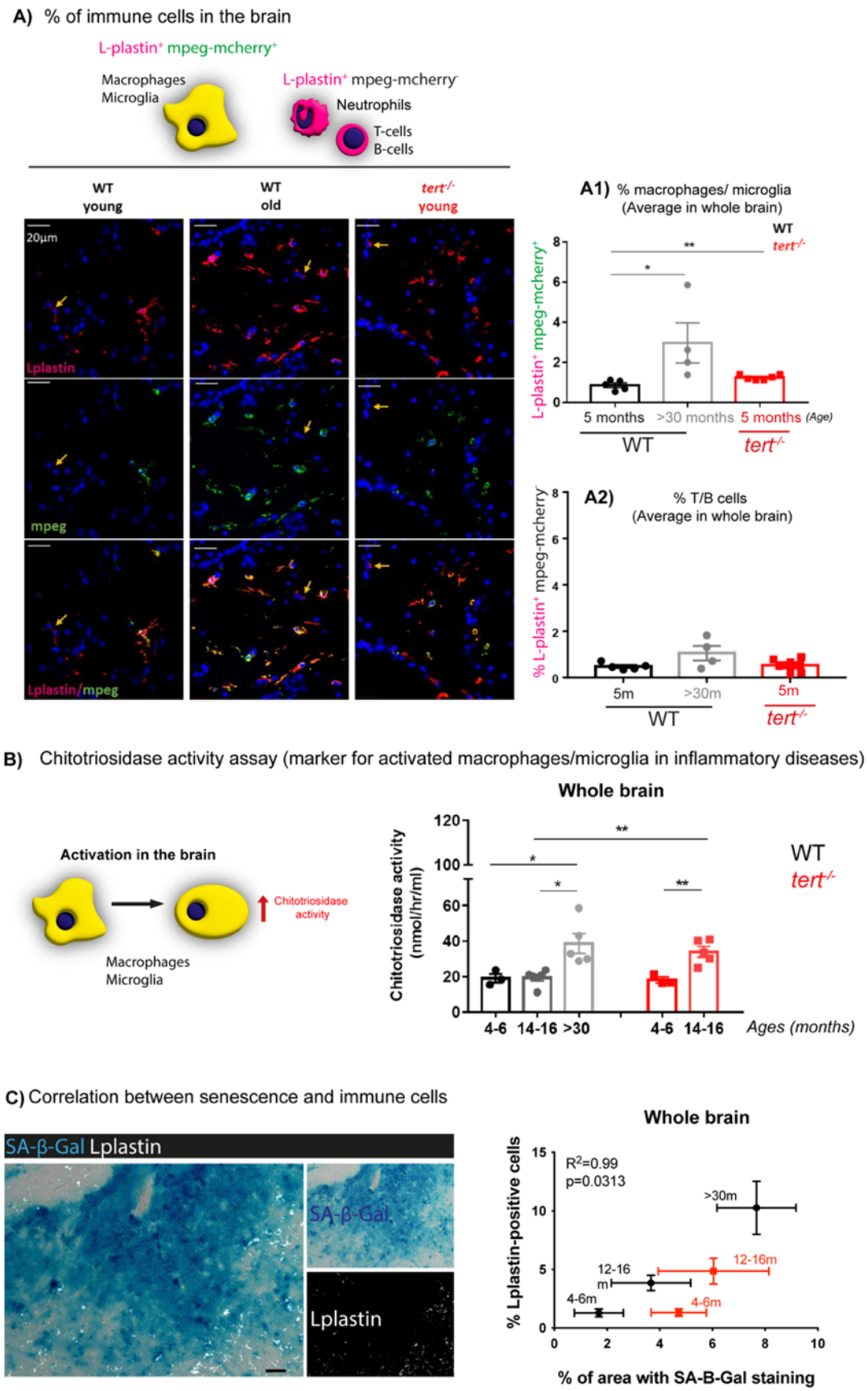

Figure 3. Telomerase (Tert)-dependent increase in inflammation with ageing in the zebrafish brain. (A) Representative images of mpeg and L-plastin staining in the diencephalon of adult zebrafish. The yellow arrow highlights a Lplastin^{+}; mpeg^{-} cell. (A1) Quantifications of L-plastin-positive; mpeg-positive cells (orange; from

505 red and green co-localisation) and (A2) L-plastin-positive; mpeg-negative cells (red) in the whole zebrafish brain
506 show an increased number of mpeg$^+$ cells with natural ageing, and this is accelerated in the absence of
507 telomerase (in *tert*$^{-/-}$ at 5 months of age). N=-6 per group. (B) Schematic figure of the chitotriosidase assay (left).
508 Chitotriosidase activity increases with natural ageing at 30 months of age, and this is accelerated in the *tert*$^{-/-}$
509 at 14-16 months (right). (C) Representative staining of SA-β-Gal (blue) and L-plastin (white) shows that most of
510 the L-plastin-positive cells do not co-localise with the SA-β-Gal staining (left). Staining quantification shows a
511 correlation between increased number of immune cells and increased expression of SA-B-Gal with ageing in
512 both WT and *tert*$^{-/-}$ (right). (A1, A2, B) Each dot represents one animal. (A1, A2, B, C) Bar errors represent the
513 SEM. * <0.05; ** <0.01; *** <0.001.
514
515 brain tissue sections. Interestingly, even though we cannot exclude that some of these
516 immune cells may also be SA-β-Gal$^+$ themselves, most of the immune cells appear as swarms
517 surrounding SA-β-Gal$^+$ areas (**Fig 3C**). Moreover, there is a statistically significant positive
518 correlation between % of SA-β-Gal$^+$ areas and % of immune cells with ageing in the WT
519 zebrafish brain (R^2=0.99), p(two-tailed) =0.0313. Importantly, this correlation seems to be
520 lost in the absence of telomerase (*tert*$^{-/-}$), where, for example, at c.5 months, the % SA-β-Gal$^+$
521 areas is more than double that of the WT at the same age and yet the % of immune cells is
522 the same. This could suggest that the inflammatory response to raised levels of senescence-
523 associated markers is deficient in the absence of telomerase. Another, not mutually exclusive
524 possibility is that *tert*$^{-/-}$ SA-β-Gal$^+$ cells are more immune evasive.
525
526 **2.4 Tert-dependent blood-brain barrier dysfunction with ageing**
527 Because our data identified a telomerase-dependent increased number of immune cells in
528 the zebrafish brain with ageing (**Fig 3A**), which was not explained by increased immune cell
529 proliferation (**Supp Fig 6**), we hypothesised that there could be immune infiltration from the
530 periphery. Immune cells should not cross the Blood Brain Barrier (BBB) and invade the brain
531 in a healthy condition unless the BBB is compromised (reviewed in (Muldoon et al., 2013)).
532 We therefore sought out to test BBB integrity in young and old zebrafish, in the presence
533 and absence of telomerase (*tert*$^{-/-}$*).*
534
535 It has been described that zebrafish have a functional BBB from the 10th day post fertilisation
536 (dpf) (Fleming, Diekmann, & Goldsmith, 2013), after which molecules such as horseradish
537 peroxidase (HRP, 44,000Da), evans blue (961Da), and sodium fluorescein (376Da) do not

538 cross this barrier (Fleming et al., 2013; Jeong et al., 2008). BBB permeability has been
539 described to increase with ageing, becoming "leaky" (Pakulski, Drobnik, & Millo, 2000) and
540 is associated with neuropathology and neuroinflammation in humans (Andjelkovic et al.,
541 2023; Knox, Aburto, Clarke, Cryan, & O'Driscoll, 2022; Sweeney, Zhao, Montagne, Nelson, &
542 Zlokovic, 2019), including in Alzheimer's disease (Bruno et al., 2024). To test whether
543 zebrafish BBB becomes leaky with ageing and whether telomerase plays a role in it, we set
544 up a BBB permeability assay in both WT and *tert*$^{-/-}$ at similar ages where increased immune
545 activation (chitotriosidase activity) was identified in the brain. To do this, we performed
546 intraperitoneal injections (IP) of an infrared fluorescent dye IRDye 680RD Dextran diluted in
547 saline (Hanks buffered solution-HBSS). We confirmed this dye's suitability for assessing BBB
548 by performing a pilot study comparing dispersion of conjugated molecules of different sizes
549 throughout the body at different time points and determined that 4kDa Dextran conjugated
550 with fluorescent dye was optimal for assessment of tissue dispersal 3 hrs post-injection
551 (**Supp Fig 7**). Three hours after injection, fish were culled, and dissected brain fluorescence
552 was measured (using a Li-cor Odyssey imaging system) to assess BBB permeability. Our data
553 show increased 4kDa dextran-FITC-associated fluorescence in the naturally aged zebrafish
554 brain at >30 months, when compared to 12 months brains, normalised to age-matched
555 vehicle (HBSS) injected animals. In the absence of telomerase (*tert*$^{-/-}$), however, there is
556 already a significant increase in dextran-associated fluorescence at 12 months when
557 compared to WT, suggesting that BBB "leakiness" increase with old age in zebrafish is a
558 telomerase-dependent phenotype and could be a means for immune cell infiltration from
559 the periphery (Deverman & Patterson, 2009).

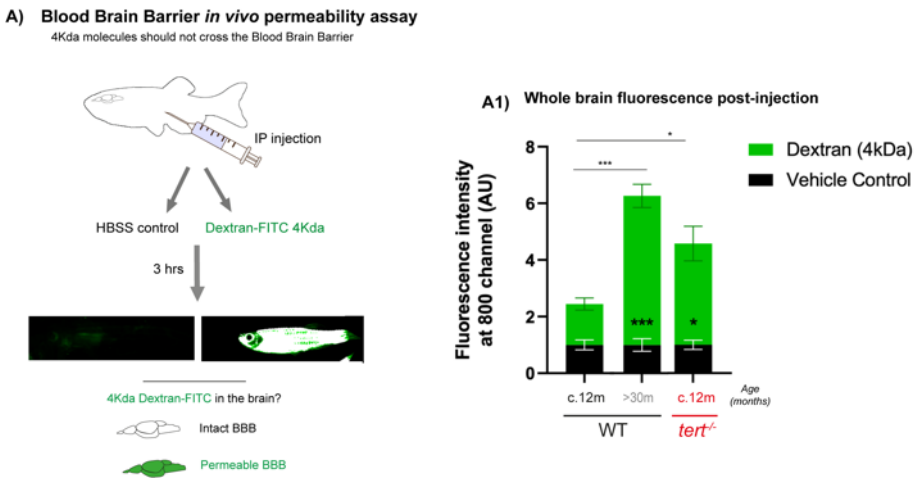

560 **Figure 4. Telomerase-dependent increased blood brain barrier permeability with ageing in the zebrafish**
561 **brain.** (A) Schematic figure of the blood brain barrier permeability assay. Dextran-FITC 4kDa or vehicle control

562 (HBSS) were injected by intraperitoneal injection and 3 hours later the fish were imaged live in the Odyssey®
563 CLx (Li-cor) to confirm the presence of Dextran-FITC in the whole body. (A1) Then the brains were dissected
564 and imaged to assess the presence of Dextran-FITC. Quantification of the green fluorescence in the fish brains
565 shows higher FITC expression in old WT (>30 months) compared to middle aged ones (12 months). This
566 increased presence of dextran-FITC in *tert*$^{-/-}$ is already observed at 12 months, overall suggesting that there is
567 increased brain permeability with natural ageing and that this is anticipated in the absence of telomerase. N=9-
568 20 per group in the tested animals; N=3-6 per group in the vehicle control animals. Bar errors represent the
569 SEM. Statistics: unpaired t-tests. * $p<0.05$; ** $p<0.01$; *** $p<0.001$.
570

571 **2.5 Tert-dependent behavioural changes with ageing**

572 It is known that inflammation can influence behaviour. For example, lipopolysaccharide
573 (LPS)-induced peripheral inflammation has been shown to lead to behavioural alterations in
574 rodents, in a dose-dependent manner, including changes in anxiety-like behaviour (Bassi et
575 al., 2012; Tarr, Chen, Wang, Sheridan, & Quan, 2012). Given that we observed a telomerase-
576 dependent increase in neuroinflammation with ageing, we set out to test whether it
577 associated with any alterations in behaviour. To do this, we assessed anxiety-like behaviour
578 using a novel object test (Maximino et al., 2010; Pegram et al., 1991; Wright, Nakamichi,
579 Krause, & Butlin, 2006), in WT and *tert*$^{-/-}$ zebrafish at young and old ages (**Fig 5A**). The novel
580 object test showed that, with ageing, WT fish tend to spend more time exploring the area
581 near the object in the centre of the tank (higher number of entries in the area next to the
582 novel object in 14-17 *versus* >30m), and this behaviour is already detected in *tert*$^{-/-}$ at the
583 earlier age of 14-17 months (**Fig 5B1**). Increased exploration of the novel object suggests
584 decreased anxiety-like behaviour with natural ageing, which our data suggest is a
585 telomerase-dependent phenotype of old age.

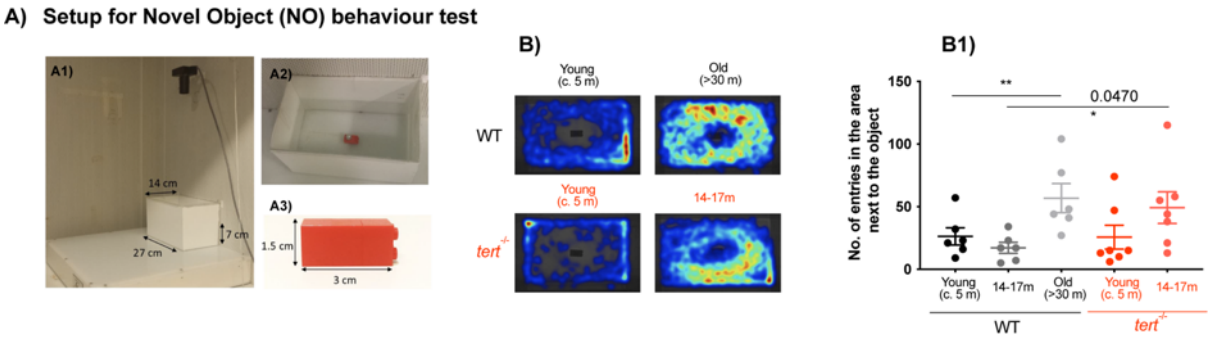

586 **Figure 5: Telomerase-dependent behaviour alterations with ageing in zebrafish.** (A) Representative images of
587 the setup used during the novel object test. (B) Heatmap representing young vs old WT and *tert*$^{-/-}$ fish
588 locomotion in the tank throughout the NO test. (B1) Quantifications show that old WT (>30 months) spend

589 longer periods of time near the novel object compared to younger siblings, and that this behaviour is already
590 observed in *tert*$^{-/-}$ at 14-17 months. N=7-9. Bar errors represent the SEM. * p<0.05; ** p<0.01; *** p<0.001
591
592 **3 DISCUSSION**
593 Brain ageing and related neurodegenerative diseases have dramatic consequences in quality
594 of life and medical care costs. Understanding the fundamental mechanisms underlying brain
595 ageing has the potential to identify therapeutic targets for multiple age-associated brain
596 diseases, which hold the promise of ameliorating quality of life in the elderly and extending
597 healthspan. Decreased telomerase expression, telomere shortening, senescence-associated
598 markers and inflammation have all been independently observed in the ageing brain and
599 associated with human neurodegeneration. However, causality between limited telomerase
600 expression and increased brain senescence and neuro-inflammation in the natural ageing
601 setting is yet to be established. Here, we address these questions using the zebrafish as an
602 ageing model which, akin to humans, displays premature ageing and death in the absence of
603 telomerase and where telomere shortening is a driver of cellular senescence. Our broad
604 transcriptomic data and enrichment analysis of whole zebrafish brains throughout the life-
605 course identified dysregulation of gene expression, stress response and dysregulation of
606 immune genes as the top 3 significantly enriched transcriptional hallmarks of old age (Frenk
607 & Houseley, 2018) in WT and these were all accelerated in the absence of telomerase (*tert*$^{-/-}$
608 *).* We decided to focus on senescence as a stress response and inflammation as proxy for
609 dysregulated immune genes, as these are amenable for further cellular and molecular
610 analysis at tissue level.
611
612 **3.1 Tert dependent increase in senescence-associated markers with ageing in the zebrafish**
613 **brain**
614 Proof of principle experiments have shown that cellular senescence is a contributor to age-
615 associated dysfunction in mice, and that selective killing of putative senescent, p16
616 expressing cells significantly ameliorated age-associated dysfunction, including cognitive
617 decline (Baker et al., 2016; Bussian et al., 2018). Further research on cellular senescence and
618 SASP have identified senolytic molecules capable removing putative senescent cells, many
619 of which are in current clinical trials, recently reviewed in (Huang et al., 2022). Importantly,
620 it is now appreciated that SASP itself plays key roles in the pathogenesis of cellular

621 senescence and SASP factors have been described to potentially contribute to the
622 "spreading" of senescence phenotypes to nearby cells, i.e, "paracrine senescence"(Acosta et
623 al., 2013). Therefore, senomorphic molecules (i.e., SASP modulating molecules) represent a
624 promising therapeutic strategy for age-related diseases. One example of such senomorphic
625 compounds is ruxolitinib, a JAK inhibitor shown to reduce putative SASP-associated
626 inflammation and alleviate frailty in old mice (Xu et al., 2015). In fact, the SASP has been
627 associated with several age-associated phenotypes including neurodegeneration (Wang et
628 al., 2024).
629
630 The transcriptional changes of old age (WT young *VS* old DEGs) that we mapped to cellular
631 senescence (enriched KEGG profile) included well-known cell signalling and cell-cycle genes
632 such *foxo1a*, *pik3*, *mapk1*, *mapk11*, multiple cyclins (*ccnd2a, ccnb3, ccnb1, ccnd1, ccna1*),
633 cyclin dependent kinases (*cdk1, cdk2, cdk6*), *chek1*, the transcription factor *e2f1*, autophagy
634 regulator sqstm1 amongst others (see supplementary data source files). We also identified
635 a number of yet to be described zebrafish genes associated with senescence to be
636 investigated in future work, namely ZGC:56235, ZGC:171775, ZFP36L1A and ZGC:114130.
637 When searching specifically for handpicked senescence-associated genes, namely *p21* and
638 *p16 (Huang et al., 2022)*, we identified *p16* as significantly up-regulated in WT aged brains
639 (WT 2m *VS* 30m, log2 fold 0.983 and p adjusted of 0.00025), which was exacerbated in the
640 absence of telomerase (tert 2m *VS* 22 months, log2 fold 1.09 and p adjusted of 0.000000002).
641 In contrast, *p21* gene expression was not significantly changed either in WT or *tert*$^{-/-}$ aged
642 brains.
643
644 Cellular senescence can be induced by different factors causing cellular impairment, including
645 DNA damage, telomere shortening or dysfunction, oncogene activation or loss of tumour
646 suppressor functions, epigenetic changes, and organelle damage, recently reviewed here
647 (Huang et al., 2022). Notably, different types of cellular senescence will express different
648 senescence-associated markers and SASP factors (Basisty et al., 2020; Hernandez-Segura et
649 al., 2018). For example, whereas DNA damage response (DDR)-induced cellular senescence is
650 often characterised by p53-p21 upregulation and pathway activation (Rossiello, Herbig,
651 Longhese, Fumagalli, & d'Adda di Fagagna, 2014), epigenetic (Petrova, Velichko, Razin, &
652 Kantidze, 2016) or mitochondria dysfunction-driven cellular senescence usually upregulates

653 p16. Moreover, p21 expression has been associated with more initial phases of cellular
654 senescence, whereas p16 seems to be involved in maintaining the senescence phenotype
655 (Dulic et al., 2000).
656
657 The most used cellular senescence-associated markers are not only the expression of p16 and
658 p21 genes but also accumulation of senescence-associated β-Galactosidase (SA- β-Gal)
659 (Huang et al., 2022). However, there is no single marker that can be exclusively and 100
660 percent relied upon to identify cellular senescence, as this likely represents a gradient of
661 phenotypes, dependent on cell type and senescence stimuli, as mentioned above (Basisty et
662 al., 2020; Hernandez-Segura et al., 2018). Acknowledging this limitation, we decided to
663 investigate the expression of several senescence-associated markers at tissue level, in aged
664 WT and *tert*$^{-/-}$ zebrafish brains. We identified an accumulation of SA-β-Gal in WT zebrafish
665 brains with ageing, which was accelerated in the absence of telomerase (*tert*$^{-/-}$). This was
666 accompanied by an increase in *p16* gene expression as assessed by RNA *in situ* hybridisation.
667 Consistent with our RNA sequencing data, we did not detect any changes in *p21* gene
668 expression as assessed by RNA *in situ* hybridisation in either WT or *tert*$^{-/-}$ aged brains. We
669 detected only a mild increase in the expression of the DDR molecule γH2AX with ageing.
670
671 Together with the fact that there were no significant changes observed in proliferation,
672 despite a decrease in telomere length in aged and *tert*$^{-/-}$ brains, and the identification of SA-
673 β-Gal in both known proliferative and non-proliferative areas of the zebrafish brain, our data
674 suggest that there is a largely DDR-independent, *p16*-dependent increase in putative
675 senescent cells in the aged zebrafish brain, which is accelerated in the absence of telomerase
676 (*tert*$^{-/-}$). Of note, even though telomere length is shorter in the *tert*$^{-/-}$ when compared to WT
677 siblings, significant even at the early age of 5 months, we did not detect significant further
678 telomere shortening from 5 to 12 months old in the *tert*$^{-/-}$. This is consistent with very low
679 levels of proliferation in the brain, but we cannot exclude the possibility that alternative
680 lengthening of telomeres (ALT) may be present, counteracting telomere shortening (Idilli et
681 al., 2020; Recagni, Bidzinska, Zaffaroni, & Folini, 2020).
682

683 Consistent with DDR-independent the SASP factors we identified in aged zebrafish brains had
684 more in common with oncogene- than genotoxic stress-induced senescence, according to
685 saspatlas.com, which has data from irradiation-induced (IR) genotoxic stress and oncogene
686 (RAS)-induced senescence in epithelial and fibroblast cells, *in vitro* (Basisty et al., 2020).
687
688 Which cells are undergoing senescence in this context remains to be determined and will
689 require future work. It has been reported that several cell populations in the CNS can undergo
690 senescence, depending on the context. Neural stem cells (NSCs) and neural progenitor cells
691 (NPCs) have been shown to undergo stress-induced senescence when exposed to ionized
692 radiation, characterised by increased SA-β-Gal (Mason, 2012) and p16 expression (Le et al.,
693 2018). Microglia, the specialised immune cells of the CNS, seem to undergo replicative
694 senescence, *in vitro* and *in vivo* (Flanary & Streit, 2004; Raj et al., 2015). *In vivo,* this was
695 demonstrated in a progeroid mice model where microglia display short telomeres and
696 modest increased expression of p21 and SASP-factors (Raj et al., 2015). Astrocytes, the most
697 abundant glial cell in the CNS, also seem to undergo stress-induced senescence, in humans
698 (Crowe et al., 2016; Mason, 2012), exhibiting high levels of SASP factors when exposed to
699 irradiation (Mason, 2012), as well as SA-β-gal activity, increased expression of DNA damage
700 checkpoints (Bitto et al., 2010) and SASP-factors (Crowe et al., 2016), when exposed to H2O2.
701 However, *in vitro* studies have reported controversial results regarding whether these cells
702 also undergo replicative senescence. Whilst Flanary & Streit (2004) did not identify replicative
703 senescence in rat astrocytes (Flanary & Streit, 2004), another two studies reported that
704 astrocytes from humans (Evans et al., 2003), mice and rats undergo replicative senescence
705 (Evans et al., 2003). Oligodendrocytes are the glial cells responsible for producing the sheath
706 of myelin around the neuronal axons. Post-mortem studies have reported increased DNA
707 damage in the white matter, together with oxidative damage and SA-β-Gal in this cell
708 population (Nasrabady et al., 2018). Importantly, neurons, considered largely non-
709 proliferative cells, have also been reported to undergo senescence. Le et al. showed increased
710 expression of p16 in the hippocampus, sub-ventricular zone (SVZ) and cortex of mice, after
711 irradiation (Le et al., 2018). Similarly, cortical neurons and Purkinje neurons of aged mice
712 present DNA damage, SA-β-Gal and SASP factors. Myenteric ganglia also undergo senescence
713 in the aged mice, presenting DNA damage, together with activated P38MAPK p38 mitogen-
714 activated protein kinases (p38MAPK), SA-β-Gal and ROS (Jurk et al., 2012). Our data show that

715 the majority of SA-β–Gal^{+} cells are not of immune origin (as assessed by L-plastin expression)
716 and are too abundant and widely distributed to be restricted to neural stem or progenitor
717 stem cells and are therefore likely to be a mixture of cell types. Future work will be required
718 to investigate this further.
719
720 **3.2 Tert-dependent neuroinflammation with ageing**
721 The Tert component of telomerase is known to play telomere-independent roles, including
722 in the modulation of mitochondria function and inflammation. Because we did not identify
723 significant changes in mitochondria complex I or II function in WT aged zebrafish brains, and
724 considering our data described so far, our current hypothesis is that non-canonical functions
725 of telomerase involved in inflammation may be contributing to the accumulation of cellular
726 senescence associated markers in the zebrafish brain, which we aim to test in future work.
727
728 Accordingly, immune dysregulation was one of the top 3 enriched ageing associated
729 transcriptomic hallmarks in both WT and *tert*$^{-/-}$ aged zebrafish brains. Furthermore, at tissue
730 level, we identified a telomerase-dependent increase in the number of
731 macrophages/microglia with ageing in the zebrafish brain. This agrees with previous
732 literature, since neuro-inflammation in humans is known to involve increased number of
733 microglia as well as increased immune activation (Damani et al., 2011; Crowe et al., 2016).
734 Similarly, two recent studies in zebrafish reported an increased number of microglia/
735 macrophages in the aged brain, more specifically in the telencephalon and optic nerve (Van
736 Houcke et al., 2017; Zambusi et al., 2020). In the telencephalon, microglia were also shown
737 to display an ameboid shape in the aged fish, suggesting increased activation (Zambusi et al.,
738 2020). Furthermore, chitotriosidase activity has been proposed as a putative marker of
739 microglial/ macrophage activation in mammals. In humans, increased levels of
740 chitotriosidase activity have been reported to increase with normal ageing (in serum)
741 (Ramanathan et al., 2013) and exacerbated in pathologies associated with chronic
742 inflammation, including in ALS (Steinacker et al., 2018). Accordingly, our data show that Tert-
743 dependent increased inflammation in the aged zebrafish brain was accompanied by
744 increased chitotriosidase activity, which is consistent with increased immune activation.
745

746 Whether this increased neuroinflammation is detrimental remains to be determined, and it
747 is not entirely clear in human neurodegeneration. Neuroinflammation is associated with
748 neurodegeneration and disease in humans (Gaikwad et al., 2024; Righi et al., 2024; Samant,
749 Standaert, & Harms, 2024), but causality is not clear. Our data show that SA-β–Gal$^+$, putative
750 senescent cells are surrounded by swarms of cells of immune origin (L-plastin$^+$) and there is a
751 significant positive correlation between increased β–Gal$^+$ areas and increased % of immune
752 cells in the brain. However, this is not the case in the absence of telomerase. For example, in
753 young *tert*$^{-/-}$ fish (c.5 months), the % SA-β-Gal$^+$ area is more than double that of the WT at the
754 same age and yet the % of immune cells is the same. This could suggest that the inflammatory
755 response to raised levels of senescence-associated markers is deficient in the absence of
756 telomerase. Our previous work identified unexpected roles for telomerase in macrophage
757 function, affecting immune activation and phagocytic ability in the zebrafish gut (Ellis et al.,
758 2022). Whether telomerase could also impact on immune recruitment and clearance of
759 senescent cells remains to be determined. Another, not mutually exclusive possibility is that
760 *tert*$^{-/-}$ SA-β-Gal$^+$ cells are more immune evasive and mechanisms similar to cancer evasion
761 from immune surveillance (Pereira et al., 2019) may be at play. Future work will be required
762 to test these hypotheses.
763
764 Finally, it is not clear whether neuroinflammation in the aged zebrafish brain is contributing
765 to the senescence phenotypes via paracrine senescence mechanisms (Acosta et al., 2013), or
766 whether immune cells are actually trying to clear senescent cells (Lujambio, 2016).
767 Nevertheless, the fact that in the absence of telomerase we have double the amount of SA-
768 β-Gal$^+$ area when compared to WT, yet the same % of immune cells as in the WT, suggests
769 that it is not inflammation that is driving it, at least in the *tert*$^{-/-}$ context. Experimental work
770 manipulating senescence and inflammation will be required to determine this. However,
771 modulating senescence and inflammation separately will present its own challenges since
772 many of the senolytic drugs currently in use also have senescence-independent anti-
773 inflammatory effects (Hernandez-Silva et al., 2022).
774
775 **3.3 Tert-dependent BBB dysfunction with ageing**
776 Our data show that neuroinflammation in the aged zebrafish brain was not explained by
777 increased levels of proliferation. We therefore hypothesised that perhaps there is increased

778 immune infiltration from the periphery due to blood brain barrier permeability or "leakiness"
779 with ageing, as has been described before with human ageing (Pakulski et al., 2000). The BBB
780 constitutes a protective barrier between the blood and the CNS, avoiding the entrance of
781 foreign molecules into the brain, including the entrance of peripheral immune cells.
782 Increased permeability can therefore lead to the infiltration of peripheral immune cells in
783 the brain (Deverman & Patterson, 2009). Moreover, the choroid plexus holds some
784 populations of resident immune cells, mostly including T-cells and monocytes but also B-
785 cells, dendritic cells and natural-killer cells (Meeker, Williams, Killebrew, & Hudson, 2012).
786 These resident immune cells have been shown to be able to invade the brain parenchyma in
787 response to inflammation (Strominger et al., 2018). Moreover, it has been described that
788 auto-reactive T-cells (Coder, Wang, Ruan, & Su, 2015) are capable of penetrating the brain
789 with ageing, both through the bloodstream and lymphatic vessels (Louveau et al., 2015).
790 Additionally, circumventricular organs constitute another mechanism by which peripheral
791 immune cells could invade the brain. These are brain structures that lack the classical BBB
792 and display high permeability (Ganong, 2000), constituting vulnerable regions to the
793 infiltration of large molecules and possibly, cells, into the brain parenchyma. Therefore,
794 increased number of immune cells in the aged brain is likely to be associated with the
795 following mechanisms: (1) increased proliferation of immune cells, particularly of microglia;
796 (2) recruitment of immune cells from the periphery, through the BBB; (3) crossing of resident
797 immune cells from the cerebrospinal fluid (choroid plexus and meninges) into the brain
798 parenchyma; and/or (4) infiltration of peripheral immune cells, through the
799 circumventricular organs.
800
801 Our data show that there is a telomerase-dependent increase in BBB permeability, therefore
802 supporting the second mechanism. However, cell tracking *in vivo* experiments would be
803 required to directly show that there is indeed immune infiltration from the periphery.
804 Mechanistically, endothelial cells and pericytes, two major components of the blood brain
805 barrier (BBB), have been reported to undergo senescence with ageing in mice, *in vitro* and *in*
806 *vivo*, expressing elevated levels of p16, p21 and SA-β-Gal (Yamazaki et al., 2016). Whether
807 BBB permeability increase with ageing in the zebrafish brain is due to endothelial senescence
808 and, if so, whether this is cell autonomous or paracrine-induced senescence remains to be
809 tested.

3.4 Tert dependent changes in anxiety like behaviour with ageing

Given that we observed a telomerase-dependent increase in neuroinflammation with ageing, and anxiety-like behaviour has previously been reported to increase in response to inflammatory stimuli (Bassi et al., 2012; Tarr et al., 2012), we sought to test whether there are telomerase-dependent behavioural changes with ageing in zebrafish. Surprisingly, against our initial hypothesis that increased inflammation would lead to increase anxiety-like behaviour, our data revealed a decrease in anxiety-like behaviour with ageing, which was accelerated in the absence of telomerase. Both age and levels of inflammation are likely to play a role in anxiety-like behaviour and interact with one another.

Anxiety-like behaviour has been reported to increase with ageing in rodents (Nolte, Nolte, & Yan, 2019) and zebrafish (Evans, Torres-Perez, Miletto Petrazzini, Riley, & Brennan, 2021; Kacprzak et al., 2017). Nonetheless, contradictory results have been observed, and this is likely to be associated with differences in animal strains used and/or differences in behaviours assessed. For example, a study in zebrafish has shown that differences in strains and specific measures assessed lead to different results in exploratory behaviour (Hudock & Kenney, 2024).

Similarly, a study in rodents (Bassi et al., 2012) has reported that anxiety-like behaviours were only detected in some of the tests performed, suggesting that the results may be variable depending on the behaviour test used and/or measures assessed. Another variable likely to influence the results is the animal age assessed, as age-associated behavioural alteration may not be linear throughout lifespan. Indeed, Ferreira et al (2023) (A. C. Ferreira, Sousa, Sousa, & Marques, 2023) observed that although there is an increase in anxiety-like behaviour in mice at 12-months of age when compared to younger mice, this was reduced later in life, at 18 months of age. In zebrafish, anxiety-like behaviour has been shown to increase with ageing, up to 18 (Evans et al., 2021; Kacprzak et al., 2017) and 24 months of age (just over "middle aged" adults) (Vasconcelos, Gordillo-Martinez, Ramos, & Lau, 2023). However, to our knowledge, our study is the first one assessing anxiety-like behaviour in old adults (i.e. >30 months old). In hand with what has been shown in mice, by Ferreira et al

841 (2023) (A. C. Ferreira et al., 2023), our study seems to suggest that there is a slight increase
842 in anxiety-like behaviour in adults (14-17 months) and a significant reduction later on in life.
843
844 Similarly to what has been reported with ageing, behaviour changes in response to
845 inflammation do not appear to be linear. Bassi et al 2012 (Bassi et al., 2012) reported a dose-
846 dependent increase in anxiety-like behaviour in response to an inflammatory stimulus, which
847 followed an inverted U curve, with slight reduced levels of anxiety-like behaviour in response
848 to intermediate doses, and increased levels of anxiety-like behaviour in response to higher
849 doses. The reduced anxiety-like behaviour we observed in old fish may be explained by
850 chronic, low levels of inflammation characteristic of ageing, in opposition to high
851 inflammatory levels of a response to an acute stimulus.
852

853 **CONCLUSIONS**

854 Our work shows for the first time that the zebrafish brain undergoes key telomerase (Tert)-
855 dependent age-associated changes at transcriptional, cellular, tissue and functional levels.
856 We show that Tert-dependent transcriptomic changes associated with dysregulation of gene
857 expression, stress response and dysregulation of immune genes are accompanied by
858 accelerated accumulation of senescence-associated markers and inflammation in the aged
859 brain. *In vivo*, these changes correlated with increased blood-brain barrier permeability and
860 altered cognitive behaviour. Together, our work suggests that telomerase has a protective
861 role in the zebrafish brain against the accumulation of senescence and neuro-inflammation
862 and is required for blood brain barrier integrity.
863

864 **MATERIALS AND METHODS**

865 **1. Animal husbandry, ethics, genotypes and ages**

866 Zebrafish were maintained at the standard conditions of 27-28ºC, in a 14:10 hour light-dark
867 cycle, and fed twice a day with Artemia (live rotifers) and Sparus (dry food). All the
868 experiments were performed in the University of Sheffield. All animal work was approved by
869 local animal review boards, including the Local Ethical Review Committee at the University
870 of Sheffield (performed according to the protocols of Project Licence 70/8681). Two strains
871 of adult zebrafish (Danio rerio) were used for these studies: wild-type (WT; AB strain) and

872 tert$^{-/(tertAB/hu3430)}$. Wild-type fish were obtained from the Zebrafish International Resource
873 Center (ZIRC). The telomerase mutant line tert $^{AB/hu3430}$ was generated by N-ethyl-nitrosourea
874 mutagenesis (Utrecht University, Netherlands (Wienholds et al., 2003)). It has a T→A point
875 mutation in the tert gene and is available at the ZFIN repository, ZFIN ID: ZDB-GENO-100412–
876 50, from ZIRC. The fish used in this study are direct descendants of the ones used in the first
877 studies describing this line(Carneiro et al., 2016; Henriques et al., 2013), by which point it
878 had been subsequently outcrossed five times with WT AB for clearing of potential
879 background mutations derived from the random ENU mutagenesis from which this line was
880 originated.
881
882 The tert $^{hu3430/hu3430}$ homozygous mutant is referred to in the paper as *tert*$^{-/-}$ and was
883 obtained by in-crossing our tert heterozygous AB/hu3430 strain, following gold standard
884 guidelines to use this line, as recently reviewed here(Henriques & Ferreira, 2024).
885 Genotyping was performed by PCR of the tert gene as before. To study age-related
886 phenotypes in the zebrafish brain, we used >30 months old fish for what we consider old in
887 WT (in the last 25-30% of their lifespan), and we considered the *tert*$^{-/-}$ old fish at the
888 equivalent age (>22 months), which approximately corresponds to the last 25-30% of their
889 lifespan. In specific, 'Old' was defined as the age at which most of the fish present age-
890 associated phenotypes, such as cachexia, loss of body mass and curvature of the spine. These
891 phenotypes develop close to the time of death and are observed at >30 months of age in WT
892 and at >22 months in *tert*$^{-/-}$ (Madalena C Carneiro et al., 2016; Henriques et al., 2013).
893 **Note on Zebrafish gene and protein nomenclature**
894 This manuscript followed the agreed convention as described in:
895 *https://zfin.atlassian.net/wiki/spaces/general/pages/1818394635/ZFIN+Zebrafish+Nomenc*
896 *lature+Conventions*
897
898 **In summary:**
899 **Gene nomenclature**
900 Genes should be named after the mammalian orthologue whenever possible. When
901 mammalian orthologues are known, the same name and abbreviation should be used,
902 except all letters are italicized and lower case. Members of a gene family are sequentially
903 numbered.

904 **Examples:**

905 Names - engrailed 1a, engrailed 2b

906 Symbols - eng1a, eng2b

907 **Protein nomenclature**

908 The protein symbol is the same as the gene symbol, but non-italic and the first letter is

909 uppercase.

910 Note the differences between zebrafish and mammalian naming conventions:

911 **species / gene / protein**

912 zebrafish /*shha*/ Shha

913 human / *SHH* / SHH

914 mouse / *Shh* / SHH

915

916 **2. Tissue fixation**

917 Paraffin-embedded sections: Fish were culled by immersion in concentrated tricaine (MS-

918 222). After terminal anaesthesia, the animals were fixed by immersion in 50 ml of 4%

919 paraformaldehyde (PFA) buffered at pH 7.0 (VWR International, Radnor, PA, USA) at 4ºC for

920 48h-72h, and decalcified in 50 ml of 0.5M ethylenediaminetetraacetic acid (EDTA), pH 8, for

921 additional 48-72h. Then, the whole fish were paraffin-embedded (in formalin I for 10min,

922 formalin II for 50min, ethanol 50% for 1h, ethanol 70% for 1h, ethanol 95% for 1h 30min,

923 ethanol 100% for 2h, ethanol 100% for 2h 30min, 50%:50% of ethanol 100% : Xilol for 1h

924 30min, xylene I for 3h, Xylene II for 3h, paraffin I for 3h, paraffin II for 4.30h), longitudinally

925 sliced (sagittal slices, 3 µm thick, using the Leica TP 1020), (3 µm thick, using the Leica TP

926 1020), and stored at room temperature (RT). To do this, diluted ethanol absolute (VWR

927 International) and paraffin histosec pastilles (Merck & Co, Kenilworth, NJ, USA) were used.

928

929 Cryosections: Fish were culled by immersion in concentrated MS-222, followed by

930 immediate decapitation (Schedule 1 method). The brain was dissected, transferred to and

931 rinsed in cold L15 (Thermo Fisher Scientific, Waltham, MA, USA). Afterwards, the brain was

932 fixed in 4% PFA (SIGMA-ALDRICH, St. Louis, MO, USA) overnight at 4°C, washed in 3ml cold

933 Phosphate Buffered Saline (PBS, 1x), and immersed in 3ml of 30% sucrose in PBS overnight

934 at 4ºC for cryoprotection. Before embedding in mounting media (O.C.T. compound, VWR

935 International), the tissues were immersed in 50%:50% solution of 30% sucrose:O.C.T. for

936 30mins at 4°C. Finally, the tissue was mounted in a base mould (Electron Microscopy
937 Sciences, Hatfield, PA, USA), with O.C.T., snap frozen, and stored at -20°C. Prior to use, the
938 tissues were sliced in 13μm-thick coronal sections using a cryostat.
939
940 **3. Immunofluorescence (IF)**
941 Paraffin sections with whole fish slices were dewaxed and hydrated through the following
942 sequence of washes: histoclear (Scientific Laboratory Supplies, Wilford, Nottingham, UK, 2x5
943 min), 100% ethanol (Thermo Fisher Scientific, 2x5 min), 90% ethanol (5 min), 70% ethanol (5
944 min), and distilled water (2x5 min). Cryosections were hydrated in PBS for 10 min before
945 proceeding. After antigen retrieval in 0.01M citrate buffer at pH 6.0 (sub-boiling at 800 W in
946 a microwave for 10 min), the tissue sections were permeabilized in PBS 0.5% Triton X-100
947 (for 10 min) and blocked in 3% bovine serum albumin (BSA), 5% Goat Serum in 0.3% Tween-
948 20 in PBS (for 1 h). Then, primary antibody incubation (overnight at 4ºC) was followed by
949 washes in PBS 0.1% Tween-20 and secondary antibody incubation (1 h at RT or overnight at
950 4ºC). Finally, the tissues were incubated in DAPI for nuclear staining (Thermo Fisher
951 Scientific), 1:10000 dilution in PBS from a 10mg/ml stock, for 10 min; washed in PBS 1x,
952 mounted with vectashield (an antifade mounting medium, from Vector Laboratories,
953 Burlingame, CA, USA), covered with coverslip (Scientific Laboratory Supplies), and sealed
954 with clear nail varnish. For details on the primary and secondary antibodies refer to Table 1
955 and Table 2, respectively.
956
957 **4. Telomere-fluorescence *in situ* hybridization (telo-FISH)**
958 Telo-FISH was performed after IF. Briefly, after incubation with the secondary antibody and
959 respective washes, the tissues were fixed in 4% PFA (SIGMA-ALDRICH) for 20min. Washes in
960 PBS, 3x 10min were followed by a dehydration step consisting of washes with ice cold 70%,
961 90% and 100% ethanol (Thermo Fisher Scientific, 3min each). After this, the slides were left
962 to dry for 1h, 10µl of hybridisation solution was pipetted on top of each tissue section and
963 the slides were covered with a coverslip. Hybridisation solution (for a total volume of 100µl):
964 8.56µl MgCl2 buffer pH 7.0, and 82mM sodium hydrogen phosphate (SIGMA-ALDRICH), 70µl
965 of deionised formamide (Thermo Fisher Scientific), 1µl of 1mM Tris, pH 7.5 (SIGMA-
966 ALDRICH), 5µl of 1x blocking buffer (10x blocking reagent (Merck & Co.) diluted to 1x in
967 maleic acid (SIGMA-ALDRICH)), 2µl of PNA probe (Telo-Cy3, zebrafish, 568; Cambridge

968 Research Biochemicals, Cleveland, UK), 2µl of Cent-Fam probe (488; Eurogentec, Liège,
969 Belgium), and 11.44µl of dH2O.
970
971 The slides were incubated for 10min at 80°C for DNA denaturation, followed by incubation
972 for 2h at RT, in the dark, to allow the probe to hybridise with the complementary DNA. After
973 the incubation period, the coverslips were gently removed and the slides were washed for
974 10min in a solution made of 70% formamide (SIGMA-ALDRICH), 10% 2x saline-sodium citrate
975 (SSC, SIGMA-ALDRICH) and 20% dH2O. This was followed by two more washes (10min each),
976 in 2x SSC. SSC was diluted from a 20x stock solution consisting of 88.3g of Tri- sodium citrate
977 dihydrate (SIGMA-ALDRICH) and 175.3g of NaCl (SIGMA-ALDRICH), diluted in dH2O to a total
978 volume of 1L, adjusted to pH of 7.0 and autoclaved. Finally, the slides were washed in PBS,
979 incubated in DAPI (Thermo Fisher Scientific) for 10min and mounted as previously described
980 in section 2.3.2.
981
982 **5. IF and telo-FISH imaging and quantification**
983 IF and telo-FISH staining was imaged using the DeltaVision microscope at the Wolfson Light
984 Microscopy Facility (LMF), using a 40x objective.t. An average of 20 images were acquired
985 from the brain of each animal (approximately 7 images per macro-area).
986 After acquisition, the images were analysed by manual counting: (1) the number of cells with
987 more than 5 foci of γH2AX (considered γH2AX+ cells) PCNA-, (2) the number of PCNA+ cells,
988 (3) the number of L-plastin+, (4) the number of mpeg+ cells, and (5) the total number of cells.
989 Telo-FISH staining was quantified by the intensity of the mean of the nucleus. The ratio
990 'telomeres/centromeres' was calculated by dividing the intensity of the mean of telomeres
991 (568 channel) by the intensity of the mean of centromeres (488 channel), which normalises
992 the telomeric probe signal by the centromeric probe signal within individual cells.
993 The analysis was performed on raw images, using the ImageJ Fiji (v. 1.51). Images were then
994 processed with Abode Illustrator 21.0.2 for display purposes.
995
996
997
998
999

1000 Table 1. Primary antibodies used for immunostaining.

Antibody, species, and type	Dilution factor	Catalogue number; company; country
PCNA mouse monoclonal	1:500	NB500-106; Novus Biologicals, Littleton, CO, USA
γH2AX, rabbit polyclonal	1:500	GTX127342; GeneTex, Irvine, CA, USA
L-plastin (Lcp1), rabbit polyclonal	1:200	GTX124420; Novus Biologicals, Littleton, CO, USA
RFP, mouse monoclonal	1:500	GTX82561; GeneTex, Irvine, CA, USA

1001

1002 Table 2. Secondary antibodies used for immunostaining.

Antibody, species, and type	Dilution factor	Catalogue number; company; country
Goat anti-rabbit IgG Alexa Fluor® 488	1:500	A11008; Invitrogen, Carlsbad, CA, USA
Goat anti-rabbit IgG Alexa Fluor® 568	1:500	10032302; Thermo Fisher Scientific, Waltham, MA, USA
Goat anti-mouse IgG Alexa Fluor® 647	1:500	A21235; Thermo Fisher Scientific, Waltham, MA, USA

1003

1004 **6. SA-β-Gal**

1005 The Senescence-Associated β-Galactosidase Staining Kit (Cell Signalling Technology, Danvers,
1006 MA, USA) was used to perform the SA-β-Gal staining, following manufacturer's instructions.
1007 Whole brain SA-β-Gal staining: Fish were culled with neat Tricaine and decapitated. Whole
1008 heads were fixed in 4ml PFA overnight at 4c with shaking. The following day, whole heads
1009 were washed 3 x for 1h in PBS at RT with slow shaking. Whole brains were then dissected in
1010 fresh PBS and immersed in 2ml in SA-β-Gal staining solution mix, consisting in 1x staining
1011 solution (pH 5.9), 1x solution A, 1x Solution B, 1mg/ml Xgal (SA-β-Gal staining kit #9860 by
1012 Cell Signaling Technology). and incubated at 37°C overnight with slow shaking in the dark.

1013 The following day, brains were washed 3 x for 1h in PBS at RT with slow shaking, and imaged
1014 using a Nikon SMZ1500 Stereomicroscope (2000).
1015 SA-β-Gal staining on cryosections: Briefly, after rinsing the cryosections in 1x PBS for 5 min,
1016 we added 200ul of β-Gal staining solution mix as above, per slide, Then, the slides were
1017 coverslipped and incubated at 37ºC overnight in a humidified chamber box. On the next day,
1018 cryosections were rinsed in 1x PBS (3x1min), and mounted in glycergel (Agilent, Santa Clara,
1019 CA, USA). Slides were then imaged using an Olympus BX60 microscope and analysed using
1020 ImageJ Fiji. Images were then processed with Abode Illustrator 21.0.2 for display purposes.
1021
1022 **7. RNA Extraction**
1023 Fish were culled by Schedule 1 method (as described before in section 2.2). Zebrafish brains
1024 were dissected, transferred to a microcentrifuge tube with 100 µl of Trizol (Thermo Fisher
1025 Scientific), snap frozen in dry ice and stored at -80ºC until RNA extraction.
1026 For RNA extraction, the tissue was homogenised with a mechanical homogenizer (VWR
1027 International) and 1.5 pestle (Kimble Chase, Vineland, NJ, USA), and an extra 50 µl of fresh
1028 Trizol (Thermo Fisher Scientific) was added. After 5 min of incubation at RT, 30 µl of
1029 chloroform (1:5, VWR International) was added. The samples were then incubated for
1030 further 3 min at RT and centrifuged (at 13,000g for 30 min at 4ºC). The resulting upper
1031 aqueous phase was transferred to a new microcentrifuge tube, and isopropanol (Thermo
1032 Fisher Scientific) was added (approximately 83% of the amount of aqueous phase). After an
1033 incubation of 10 min at RT, the samples were centrifuged (13,000g for 15 min at 4ºC) and
1034 the supernatant was discarded. The pellets were washed in 250 µl of 75% ethanol twice and
1035 then left to air dry. In the end, the pellets were resuspended in 14 µl of nuclease-free water
1036 (VWR International) and stored at -80ºC. All the samples were analysed by Nanodrop 1000
1037 Spectrophotometer to measure the concentration of RNA. Some samples (randomly chosen)
1038 were also analysed in the Bioanalyzer to assess RNA integrity. All the samples included in this
1039 study had an RNA integrity number (RIN) of >9.
1040
1041 **8. RNA sequencing**
1042 RNA-Sequencing was performed at the Genomics and Sequencing facility of Sheffield
1043 Institute for Translational Neuroscience (SITraN). Mature RNA was isolated and fragmented
1044 using the NEBNext Poly(A) mRNA Magnetic Isolation Module (New England Biolabs Inc),

1045 following manufacturer's instructions. The libraries were prepared using the NEBNext Ultra
1046 Directional RNA Library Prep Kit (Illumina), following manufacturer's instructions. The
1047 NEBNext Multiplex Oligos from Illumina (Index Primers Set 1, New England Biolabs Inc) was
1048 used for the library preparation using the following PCR program: 98ºC for 30 sec (1 cycle),
1049 98ºC for 10 sec followed by 65ºC for 75 sec (8 cycles), and 65ºC for 5min. The PCR product
1050 (≈50µl) was then purified using 45µl of Oligo dT Beads (Agencourt AMPure XP), followed by
1051 three washes with ethanol 80%. After air-drying, the dscDNA was eluted by adding 23µl of
1052 0.1x TE, and the resulting 20µl of the library were collected. Sequencing was run on an
1053 Illumina HiScan SQ sequencer, using a high output run and sequencing by synthesis V3
1054 chemistry on a single 100 base pair (bp) run. The sequencing process was monitored in real-
1055 time using Sequencing Analysis Viewer v1.8.37 Software, and therefore quality control was
1056 performed during and after sequencing. Then, the data was imported into a FASTA file
1057 format to perform the analysis.
1058
1059 **9. RNA Sequencing analysis**
1060 Data processing:
1061 Quality control was performed using MultiQC version 1.9.Cutadapt version 3.0 was used for
1062 trimming the first 13 bases from the reads to remove poor quality base pairs in the reads.
1063 Read alignment was performed as follows. Single-end reads were aligned against the
1064 reference genome Danio_rerio.GRCz11.dna. primary_assembly.fa using STAR. A bespoke
1065 alignment index was built using annotation file Danio_rerio.GRCz11.103.gtf and an expected
1066 read length of 88bp. Ht-seq count was run in non-stranded mode to obtain per gene read
1067 counts.
1068 Differential expression: To identify signatures of ageing, WT brain samples were subjected
1069 separately to DESEq2 analysis, comparing the time points 9, 22 and >30 months with the
1070 time-point of 2 months. Then, *tert*$^{-/-}$ samples at 2, 9 and 22 months were compared with WT
1071 at 2 months, to identify telomerase-dependent ageing processes.
1072 Enrichment analysis: Pathway enrichment analysis was performed using the Functional
1073 Annotation Bioinformatics Microarray Analysis programme (https://david.ncifcrf.gov/).
1074 Pathways identified in both Gene Ontology Biological Process (GO-BP) and KEGG databases
1075 were included in the analysis. The top 10 GO-BP and KEGG terms were then plotted into a
1076 heatmap using graphpad Prism.

1077 Mapping to the hallmarks of ageing: We analysed the recent Frenk & Houseley's paper (Frenk
1078 & Houseley, 2018), which describes the different transcriptional hallmarks of aging. In this
1079 paper, the different hallmarks are defined within specific text sections. For each hallmark,
1080 we collected groups of keywords that could be within GO term names. The complete list of
1081 GO term names was extracted from the file go-basic.obo from the Gene Ontology website
1082 (https://geneontology.org/). We then established lists of GO term names for each
1083 transcriptional hallmark of aging. The mapping table between the hallmarks, the keywords,
1084 and the lists of GO term names is available in the table GO_to_HA-THA_V1.csv.
1085
1086 Zebrafish genes and their associated GO term names were retrieved from the mapping
1087 function Gene2GoReader() from the Python library goatools. We built 3 distinct dictionaries
1088 for each GO category (Biological Process, Molecular Function, and Cellular Component),
1089 where the entrezgene IDs are associated with their GO term names. From the differential
1090 analyses, we obtained different lists of gene symbols that must first be mapped to
1091 entrezgene ID, using the Python library mygene. Each gene ID is associated with a list of GO
1092 term names. To assess a particular transcriptional hallmark of aging to a given gene, we
1093 parsed their associated list of GO term names and mapped them to their corresponding
1094 hallmark of aging.
1095
1096 Depending on the situation, the attribution of the hallmark of ageing is done as follows: 1)
1097 all the GO term names are mapped to the same transcriptional hallmark of ageing, 2) the GO
1098 term names are mapped to several transcriptional hallmarks of ageing, the hallmark with the
1099 highest number of occurrence is chosen. Otherwise, the gene is assigned with an
1100 "ambiguous" hallmark of ageing if 3) none of the GO term names are mapped to any
1101 transcriptional hallmarks of ageing, then the gene is not annotated with a transcriptional
1102 hallmark of aging.
1103
1104 **10. Protein extraction and quantification**
1105 Fish were culled by Schedule 1 method as previously described. Brain tissue was dissected,
1106 transferred to a microcentrifuge tube and immediately snap-frozen in liquid nitrogen. The
1107 samples were stored at -80°C until protein extraction.

1108 The tissue was homogenised in 100µl of ultra-pure water using a mechanical homogenizer
1109 (VWR International) and RNAse-free disposable pestles (Thermo Fisher Scientific) for
1110 approximately 30sec, on ice. Then, the samples were spun down at 4°C, at 2,000rpm, for
1111 5min. After transferring the supernatant to a new tube, samples were stored at -80°C until
1112 further use.
1113
1114 Protein extracts were quantified by the bicinchoninic acid (BCA) method, using the Pierce™
1115 BCA Protein Assay Kit (Thermo Fisher Scientific), following manufacturer's instructions.
1116 Briefly, a standard curve was prepared with a range of 0.2-2µm of BSA, along with a blank
1117 control (containing ultra-pure water only). A total of 5µl of each protein extract was mixed
1118 with 1ml of BCA, in microcentrifugation tubes, and incubated at 37°C for 10min in a water
1119 bath. After adding an additional 20µl of copper sulphate, the solution was mixed and
1120 incubated at 37°C for 20min. Then, 200µl of each sample (or BSA standard curve) were
1121 transferred to a Corning™ Costar™ Brand 96-Well EIA/RIA Plate (Thermo Fisher Scientific), in
1122 duplicates, and absorbances were read in a Varioskan Plate Reader at a wavelength of
1123 562nm.
1124
1125 **11. Chitotriosidase activity assay**
1126 Chitotriosidase activity was measured using the protocol previously described by Keatinge
1127 et al., (2015). This method allows assessment of the hydrolysis capacity of 4–
1128 methylumbelliferyl–β-D-N, N', N"-triacetylchitotriose (4-MU-chitotrioside), by
1129 chitotriosidase enzyme.
1130
1131 Briefly, a total of 10µl of protein extract per sample was mixed with 100µl of substrate
1132 solution and incubated at 28°C for 6 min. A blank control containing 10µl of ultra-pure water
1133 was prepared alongside the samples. Substrate solution consisted in 4-MU-chitotrioside
1134 (SIGMA-ALDRICH) diluted in McIlvaine solution at pH 5.2 (1.73mg of 4-MU-chitotrioside per
1135 100 ml of McIlvaine solution). To make the McIlvaine solution, stock solutions of 0.1M citric
1136 acid (SIGMA-ALDRICH) and 0.2M di-sodium hydrogen phosphate (SIGMA-ALDRICH) were
1137 mixed at a ratio of 45% and 55%, respectively, obtaining a final pH of 5.2. After incubation,
1138 1ml of stop solution (0.25M glycine buffer, pH 10.4, containing 0.01% Triton X-100 (SIGMA-
1139 ALDRICH) was added to each sample (and blank control), and 200µl of the final solution was

1140 transferred to a Corning™ Costar™ Brand 96-Well EIA/RIA Plate (Thermo Fisher Scientific).
1141 Duplicates of each sample were used. An extra microcentrifuge tube was prepared with
1142 200µl of standard solution (5µm 1,4-Methylumbelliferone, SIGMA-ALDRICH) and 900µl of
1143 stop solution. A volume of 200µl of the final solution was transferred to the 96-well plate, in
1144 duplicates. The fluorescence was then read in a Varioskan Plate Reader (excitation: 365nm;
1145 emission: 450nm). Finally, the chitotriosidase activity was calculated in nM/h/ml, using
1146 Formula 4.
1147
1148 **T**, fluorescence of test samples
1149 **B**, fluorescence of blank
1150 **Std**, standard

1151 $$\frac{(\boldsymbol{T}-\boldsymbol{B})}{\boldsymbol{std}} x \frac{60}{incubation\ time\ [min]} x \frac{1000}{volume\ [\mu l]}$$

1152
1153 **12. Blood Brain Barrier (BBB) permeability assay**
1154 To test BBB permeability, a total of 5µl of 0.1% IRDye 680RD Dextran (LI-COR Biosciences,
1155 Lincoln, NE, USA) diluted in HBSS (Thermo Fisher Scientific) were injected by intraperitoneal
1156 injection (IP). Two different sizes of the compound were tested, with the following molecular
1157 weights: 4kDa and 70kDa. A group of fish injected with 5µl of HBSS alone was used as a
1158 vehicle control group. The fish were culled 3h after IP, and the brains were collected and
1159 imaged using a LI-COR Odyssey CLx machine (LI-COR). The brain fluorescence was then
1160 quantified using the Image Studio 4.0 Software for Odyssey CLx (LI-COR).
1161
1162 **13. Mitochondrial complex assays**
1163 Homogenised brain tissue was diluted to approximately 0.7mg protein/ml and subjected to
1164 3 cycles of rapid freeze-thawing in liquid nitrogen. All spectrophotometric assays were
1165 performed at 28°C in 200µl final volume using a Fluostar Omega plate reader. For assessing
1166 complex I activity, the assay buffer was 25mM KH_2PO_4, 5mM $MgCl_2$, (pH7.2), 3mM KCN,
1167 2.5mg/ml BSA, 50µM ubiquinone, 2µg/ml antimycin A. Complex I activity was determined by
1168 measuring the oxidation of nicotinamide adenine dinucleotide reduced disodium salt
1169 (NADH) at 340nm with a reference wavelength of 425nm (ε = 6.22mM^{-1} cm^{-1}). 125µM NADH
1170 started the reaction, and 3µg/ml rotenone was used to inhibit the reaction. For assessing

1171 Complex II activity the brain homogenate was incubated for 10min in assay buffer containing
1172 25mM KH_2PO_4, 5mM $MgCl_2$, (pH 7.2), 3mM KCN, 20 mM succinate. 50µM 2,6-DCPIP, 2µg/ml
1173 antimycin A and 3µg/ml rotenone were then added, and baseline measurements recorded.
1174 The reaction was started with the addition of 50µM ubiquinone Q1 and complex II activity
1175 determined by measuring the reduction of 2,6-dichlorobenzenone-indophenol sodium salt
1176 (2,6-DCPIP) at 600nm (ε = 19.2mM^{-1} cm^{-1}). Complex I and complex II activity rates are
1177 normalised to citrate synthase activity.
1178
1179 **14. Novel object (NO) test**
1180 Before the experiment, all fish were acclimatised to the behaviour room for at least 1h. The
1181 NO test was performed using a 27x14x14cm tank (length x width x height) containing 7cm of
1182 water depth, with a red 3x1.5x1.5cm object (length x width x height) placed in the centre.
1183 The walls of the test tank were covered in white paper to avoid external visual stimuli. A fish
1184 was gently placed into the test tank with a net and the recording of the test behaviour started
1185 immediately, using a top camera, for a total period of 10min. In the end, the fish was
1186 returned to its tank. The water in the test tank was replaced in between every fish. The assay
1187 was performed for 3 consecutive days and 10 to 20 fish were tested per day. The day and
1188 time of experiment were semi-randomly determined so that all the fish from each group
1189 were equally distributed for the morning and afternoon sessions of each day of experiment
1190 to avoid confounding factors related to the day and schedule of the experiment. Later, fish
1191 behaviour was analysed using the video tracking software EthoVision® XT (Noldus
1192 Information Technology Inc., Lessburg, VA, USA). Anxiety-like behaviour was measured by
1193 the number of entries in the areanear the novel object. Two times the width of the fish was
1194 the measure used to delimit the area considered to be 'near the object'.
1195
1196 **15. Statistical analysis**
1197 All the graphs and respective statistical analysis were performed with GraphPad Prism 7.0.
1198 Normality was assessed by comparing group variances using either the Brown-Forsythe test
1199 or the Shapiro-Wilk normality test. Unpaired t-test or Mann Whitney's unpaired t-test were
1200 used to compare 2 groups, depending on whether the samples presented a Gaussian
1201 distribution or not, respectively. For groups with normal distribution, comparisons over-time
1202 were performed using ANOVA, followed by Turkey test for multiple comparisons. For groups

1203 that failed the normality tests, non-parametric tests were performed, followed by Dunnett's
1204 test for multiple comparisons. A critical value for significance of $p<0.05$ was used in all the
1205 analysis.
1206

1207 **ACKNOWLEDGEMENTS**

1208 We would like to acknowledge and thank Dr Marcus Keatinge for helping with the
1209 chitotriosidase activity assay. We would like to acknowledge and thank Dr William Norton
1210 from the University of Leicester for kindly allowing us to use his EthoVision® XT software
1211 (Noldus). We would like to acknowledge and thank the University of Sheffield Aquarium staff
1212 for the great care they provide to our fish and help with protocols, fish selection and
1213 breeding. We would like to acknowledge and thank the Wolfson Light Microscopy Facility
1214 staff for their support throughout the years with all our imaging needs and challenges.

1215 This work was generously funded by a University of Sheffield PhD studentship to RRM. This
1216 research was funded in whole, or in part, by Wellcome [206224/Z/17/Z/WT_/Wellcome
1217 Trust/United Kingdom]. For the purpose of open access, the author has applied a CC BY
1218 public copyright licence to any Author Accepted Manuscript version arising from this
1219 submission. CMH was also funded by a Vice Chancellor's Fellowship, The University of
1220 Sheffield and a Dunhill Medical Trust grant AISRPG2305\32, which cover PSE salary.

1221 MR is funded by the CNRS and the ANR ADAGIO (ANR-20-CE44-0010). Thanks to the
1222 Bettencourt Schueller Foundation long-term partnership, this work was partly supported by
1223 the CRI Core Research Fellowship to Michael Rera for SB salary.

1224

1225 **CONFLICT OF INTEREST**

1226 The authors declare no competing interests.

1227

1228 **AUTHOR CONTRIBUTIONS**

1229 *Author contributions according to CRediT:*

1230 **RRM**: conceptualisation, data curation, formal analysis, funding acquisition, investigation,
1231 methodology, project administration, validation, visualisation, writing

SB: data curation, formal analysis, investigation, methodology, software, validation, visualisation, writing

PSE: data curation, formal analysis, investigation, methodology, validation, writing

NH: data curation, formal analysis, investigation, methodology

NM: investigation

OE: investigation

MHFW: investigation

ZY: investigation

HM: data curation, formal analysis, funding acquisition, investigation, methodology

MR: data curation, formal analysis, funding acquisition, investigation, methodology, project administration, software, validation, visualisation, writing

CMH: conceptualisation, data curation, formal analysis, funding acquisition, investigation, methodology, project administration, resources, supervision, validation, writing

DATA AVAILABILITY STATEMENT

The dataset and source data generated during and/or analysed during the current study is either shared as supplementary and source data or is available from the corresponding author upon reasonable request. The RNA sequencing data from this experiment were deposited in gene expression omnibus (GEO) and will be made available when in peer review.

ORCID

Raquel R. Martins: https://orcid.org/0000-0003-3952-8649

Savandara Besse: https://orcid.org/0000-0003-2448-4022

Pam S. Ellis: https://orcid.org/0000-0002-5915-4739

Naomi Hartopp: https://orcid.org/0000-0003-4069-6324

Owain Evans: https://orcid.org/0009-0000-8493-4983

Heather Mortiboys: https://orcid.org/0000-0001-6439-0579

Michael Rera: https://orcid.org/0000-0002-6574-6511

Catarina M. Henriques: https://orcid.org/0000-0003-1882-756X

TOTAL CHARACTERS WITH SPACES: 87566 (includes figure legends. For final submission we will move most of the details in methodology to supplementary information)

REFERENCES

Acosta, J. C., Banito, A., Wuestefeld, T., Georgilis, A., Janich, P., Morton, J. P., . . . Gil, J. (2013). A complex secretory program orchestrated by the inflammasome controls paracrine senescence. *Nat Cell Biol, 15*(8), 978-990. doi:10.1038/ncb2784

Ahmed, S., Passos, J. F., Birket, M. J., Beckmann, T., Brings, S., Peters, H., . . . Saretzki, G. (2008). Telomerase does not counteract telomere shortening but protects mitochondrial function under oxidative stress. *J Cell Sci, 121*(Pt 7), 1046-1053. doi:10.1242/jcs.019372

Anchelin, M., Alcaraz-Perez, F., Martinez, C. M., Bernabe-Garcia, M., Mulero, V., & Cayuela, M. L. (2013). Premature aging in telomerase-deficient zebrafish. *Dis Model Mech, 6*(5), 1101-1112. doi:10.1242/dmm.011635

Andjelkovic, A. V., Situ, M., Citalan-Madrid, A. F., Stamatovic, S. M., Xiang, J., & Keep, R. F. (2023). Blood-Brain Barrier Dysfunction in Normal Aging and Neurodegeneration: Mechanisms, Impact, and Treatments. *Stroke, 54*(3), 661-672. doi:10.1161/STROKEAHA.122.040578

Baker, D. J., Childs, B. G., Durik, M., Wijers, M. E., Sieben, C. J., Zhong, J., . . . van Deursen, J. M. (2016). Naturally occurring p16(Ink4a)-positive cells shorten healthy lifespan. *Nature, 530*(7589), 184-189. doi:10.1038/nature16932

Basisty, N., Kale, A., Jeon, O. H., Kuehnemann, C., Payne, T., Rao, C., . . . Schilling, B. (2020). A proteomic atlas of senescence-associated secretomes for aging biomarker development. *PLoS Biol, 18*(1), e3000599. doi:10.1371/journal.pbio.3000599

Bassi, G. S., Kanashiro, A., Santin, F. M., de Souza, G. E., Nobre, M. J., & Coimbra, N. C. (2012). Lipopolysaccharide-induced sickness behaviour evaluated in different models of

1289 anxiety and innate fear in rats. *Basic Clin Pharmacol Toxicol, 110*(4), 359-369.
1290 doi:10.1111/j.1742-7843.2011.00824.x
1291 Bhat, R., Crowe, E. P., Bitto, A., Moh, M., Katsetos, C. D., Garcia, F. U., . . . Torres, C. (2012).
1292 Astrocyte senescence as a component of Alzheimer's disease. *PLoS One, 7*(9), e45069.
1293 doi:10.1371/journal.pone.0045069
1294 Birch, J., & Gil, J. (2020). Senescence and the SASP: many therapeutic avenues. *Genes Dev,*
1295 *34*(23-24), 1565-1576. doi:10.1101/gad.343129.120
1296 Blackburn, E. H., Epel, E. S., & Lin, J. (2015). Human telomere biology: A contributory and
1297 interactive factor in aging, disease risks, and protection. *Science, 350*, 1193-1198.
1298 doi:10.1126/science.aab3389
1299 Bodnar, A. G. (1998). Extension of Life-Span by Introduction of Telomerase into Normal
1300 Human Cells. *Science, 279*(5349), 349-352. doi:10.1126/science.279.5349.349
1301 Bruno, M., Bonomi, C. G., Ricci, F., Di Donna, M. G., Mercuri, N. B., Koch, G., . . . Motta, C.
1302 (2024). Blood-brain barrier permeability is associated with different
1303 neuroinflammatory profiles in Alzheimer's disease. *Eur J Neurol, 31*(1), e16095.
1304 doi:10.1111/ene.16095
1305 Bussian, T. J., Aziz, A., Meyer, C. F., Swenson, B. L., van Deursen, J. M., & Baker, D. J. (2018).
1306 Clearance of senescent glial cells prevents tau-dependent pathology and cognitive
1307 decline. *Nature, 562*(7728), 578-582. doi:10.1038/s41586-018-0543-y
1308 Cao, Y., Li, H., Deb, S., & Liu, J. P. (2002). TERT regulates cell survival independent of
1309 telomerase enzymatic activity. *Oncogene, 21*(20), 3130-3138.
1310 doi:10.1038/sj.onc.1205419
1311 Carneiro, M. C., Henriques, C. M., Nabais, J., Ferreira, T., Carvalho, T., & Ferreira, M. G. (2016).
1312 Short Telomeres in Key Tissues Initiate Local and Systemic Aging in Zebrafish. *PLoS*
1313 *Genetics, 12*, e1005798. doi:10.1371/journal.pgen.1005798
1314 Chinta, S. J., Woods, G., Demaria, M., Rane, A., Zou, Y., McQuade, A., . . . Andersen, J. K. (2018).
1315 Cellular Senescence Is Induced by the Environmental Neurotoxin Paraquat and
1316 Contributes to Neuropathology Linked to Parkinson's Disease. *Cell Rep, 22*(4), 930-
1317 940. doi:10.1016/j.celrep.2017.12.092
1318 Choi, J., Southworth, L. K., Sarin, K. Y., Venteicher, A. S., Ma, W., Chang, W., . . . Artandi, S. E.
1319 (2008). TERT promotes epithelial proliferation through transcriptional control of a

1320 Myc- and Wnt-related developmental program. *PLoS Genet, 4*(1), e10.
1321 doi:10.1371/journal.pgen.0040010
1322 Coder, B. D., Wang, H., Ruan, L., & Su, D. M. (2015). Thymic involution perturbs negative
1323 selection leading to autoreactive T cells that induce chronic inflammation. *J Immunol,*
1324 *194*(12), 5825-5837. doi:10.4049/jimmunol.1500082
1325 Collins, B., Bandosz, P., Guzman-Castillo, M., Pearson-Stuttard, J., Stoye, G., McCauley, J., . . .
1326 O'Flaherty, M. (2022). What will the cardiovascular disease slowdown cost? Modelling
1327 the impact of CVD trends on dementia, disability, and economic costs in England and
1328 Wales from 2020-2029. *PLoS One, 17*(6), e0268766.
1329 doi:10.1371/journal.pone.0268766
1330 Coppe, J. P., Desprez, P.-Y. Y., Krtolica, A., Campisi, J., Coppé, J.-P., Desprez, P.-Y. Y., . . .
1331 Campisi, J. (2010). The senescence-associated secretory phenotype: the dark side of
1332 tumor suppression. *Annual review of pathology, 5*, 99-118. doi:10.1146/annurev-
1333 pathol-121808-102144
1334 Cvejic, A., Hall, C., Bak-Maier, M., Flores, M. V., Crosier, P., Redd, M. J., & Martin, P. (2008).
1335 Analysis of WASp function during the wound inflammatory response--live-imaging
1336 studies in zebrafish larvae. *J Cell Sci, 121*(Pt 19), 3196-3206. doi:10.1242/jcs.032235
1337 d'Adda di Fagagna, F., Reaper, P. M., Clay-Farrace, L., Fiegler, H., Carr, P., Von Zglinicki, T., . . .
1338 Jackson, S. P. (2003). A DNA damage checkpoint response in telomere-initiated
1339 senescence. *Nature, 426*(6963), 194-198. doi:10.1038/nature02118
1340 De Felice, B., Annunziata, A., Fiorentino, G., Manfellotto, F., D'Alessandro, R., Marino, R., . . .
1341 Biffali, E. (2014). Telomerase expression in amyotrophic lateral sclerosis (ALS)
1342 patients. *J Hum Genet, 59*(10), 555-561. doi:10.1038/jhg.2014.72
1343 de Lange, T. (2004). T-loops and the origin of telomeres. *Nature reviews. Molecular cell*
1344 *biology, 5*, 323-329. doi:10.1038/nrm1422
1345 Deacon, K., & Knox, A. J. (2018). PINX1 and TERT Are Required for TNF-alpha-Induced Airway
1346 Smooth Muscle Chemokine Gene Expression. *J Immunol, 200*(4), 1283-1294.
1347 doi:10.4049/jimmunol.1700414
1348 Deleidi, M., Jäggle, M., & Rubino, G. (2015). Immune aging, dysmetabolism, and inflammation
1349 in neurological diseases. *Frontiers in neuroscience, 9*, 172.
1350 doi:10.3389/fnins.2015.00172

1351 Deverman, B. E., & Patterson, P. H. (2009). Cytokines and CNS development. *Neuron, 64*(1),
1352 61-78. doi:10.1016/j.neuron.2009.09.002
1353 Dimri, G. P., Lee, X., Basile, G., Acosta, M., Scott, G., Roskelley, C., . . . et al. (1995). A biomarker
1354 that identifies senescent human cells in culture and in aging skin in vivo. *Proc Natl*
1355 *Acad Sci U S A, 92*(20), 9363-9367.
1356 Dulic, V., Beney, G. E., Frebourg, G., Drullinger, L. F., & Stein, G. H. (2000). Uncoupling between
1357 phenotypic senescence and cell cycle arrest in aging p21-deficient fibroblasts. *Mol Cell*
1358 *Biol, 20*(18), 6741-6754. doi:10.1128/MCB.20.18.6741-6754.2000
1359 Eitan, E., Tichon, A., Gazit, A., Gitler, D., Slavin, S., & Priel, E. (2012). Novel telomerase-
1360 increasing compound in mouse brain delays the onset of amyotrophic lateral sclerosis.
1361 *EMBO Mol Med, 4*(4), 313-329. doi:10.1002/emmm.201200212
1362 Ellett, F., Pase, L., Hayman, J. W., Andrianopoulos, A., & Lieschke, G. J. (2011). mpeg1
1363 promoter transgenes direct macrophage-lineage expression in zebrafish. *Blood,*
1364 *117*(4), e49-56. doi:10.1182/blood-2010-10-314120
1365 Ellis, P. S., Martins, R. R., Thompson, E. J., Farhat, A., Renshaw, S. A., & Henriques, C. M. (2022).
1366 A subset of gut leukocytes has telomerase-dependent "hyper-long" telomeres and
1367 require telomerase for function in zebrafish. *Immun Ageing, 19*(1), 31.
1368 doi:10.1186/s12979-022-00287-8
1369 Evans, J. R., Torres-Perez, J. V., Miletto Petrazzini, M. E., Riley, R., & Brennan, C. H. (2021).
1370 Stress reactivity elicits a tissue-specific reduction in telomere length in aging zebrafish
1371 (Danio rerio). *Sci Rep, 11*(1), 339. doi:10.1038/s41598-020-79615-1
1372 Ferreira, A. C., Sousa, N., Sousa, J. C., & Marques, F. (2023). Age-related changes in mice
1373 behavior and the contribution of lipocalin-2. *Front Aging Neurosci, 15*, 1179302.
1374 doi:10.3389/fnagi.2023.1179302
1375 Ferreira, M. G., Miller, K. M., & Cooper, J. P. (2004). Indecent exposure: when telomeres
1376 become uncapped. *Mol Cell, 13*(1), 7-18.
1377 Fleming, A., Diekmann, H., & Goldsmith, P. (2013). Functional characterisation of the
1378 maturation of the blood-brain barrier in larval zebrafish. *PLoS One, 8*(10), e77548.
1379 doi:10.1371/journal.pone.0077548
1380 Forsyth, N. R., Wright, W. E., & Shay, J. W. (2002). Telomerase and differentiation in
1381 multicellular organisms: turn it off, turn it on, and turn it off again. *Differentiation,*
1382 *69*(4-5), 188-197. doi:10.1046/j.1432-0436.2002.690412.x

1383 Franceschi, C., & Campisi, J. (2014). Chronic inflammation (inflammaging) and its potential
1384 contribution to age-associated diseases. *J Gerontol A Biol Sci Med Sci, 69 Suppl 1*, S4-
1385 9. doi:10.1093/gerona/glu057
1386 Frenk, S., & Houseley, J. (2018). Gene expression hallmarks of cellular ageing. *Biogerontology,*
1387 *19*(6), 547-566. doi:10.1007/s10522-018-9750-z
1388 Fridlyanskaya, I., Alekseenko, L., & Nikolsky, N. (2015). Senescence as a general cellular
1389 response to stress: A mini-review. *Exp Gerontol, 72*, 124-128.
1390 doi:10.1016/j.exger.2015.09.021
1391 Gaikwad, S., Senapati, S., Haque, M. A., & Kayed, R. (2024). Senescence, brain inflammation,
1392 and oligomeric tau drive cognitive decline in Alzheimer's disease: Evidence from
1393 clinical and preclinical studies. *Alzheimers Dement, 20*(1), 709-727.
1394 doi:10.1002/alz.13490
1395 Ganong, W. F. (2000). Circumventricular organs: definition and role in the regulation of
1396 endocrine and autonomic function. *Clin Exp Pharmacol Physiol, 27*(5-6), 422-427.
1397 doi:10.1046/j.1440-1681.2000.03259.x
1398 Ghosh, A., Saginc, G., Leow, S. C., Khattar, E., Shin, E. M., Yan, T. D., . . . Tergaonkar, V. (2012).
1399 Telomerase directly regulates NF-kappaB-dependent transcription. *Nat Cell Biol,*
1400 *14*(12), 1270-1281. doi:10.1038/ncb2621
1401 Gomes, N. M. V., Ryder, O. a., Houck, M. L., Charter, S. J., Walker, W., Forsyth, N. R., . . . Wright,
1402 W. E. (2011). Comparative biology of mammalian telomeres: hypotheses on ancestral
1403 states and the roles of telomeres in longevity determination. *Aging Cell, 10*, 761-768.
1404 doi:10.1111/j.1474-9726.2011.00718.x
1405 Goodman, W. A., & Jain, M. K. (2011). Length does not matter: A new take on telomerase
1406 reverse transcriptase. *Arteriosclerosis, Thrombosis, and Vascular Biology, 31*, 235-236.
1407 doi:10.1161/ATVBAHA.110.220343
1408 Haendeler, J., Drose, S., Buchner, N., Jakob, S., Altschmied, J., Goy, C., . . . Dimmeler, S. (2009).
1409 Mitochondrial telomerase reverse transcriptase binds to and protects mitochondrial
1410 DNA and function from damage. *Arterioscler Thromb Vasc Biol, 29*(6), 929-935.
1411 doi:10.1161/ATVBAHA.109.185546
1412 Henriques, C. M., Carneiro, M. C., Tenente, I. M., Jacinto, A., & Ferreira, M. G. (2013).
1413 Telomerase is required for zebrafish lifespan. *PLoS Genet, 9*(1), e1003214.
1414 doi:10.1371/journal.pgen.1003214

1415 Henriques, C. M., & Ferreira, M. G. (2012). Consequences of telomere shortening during
1416 lifespan. *Curr Opin Cell Biol, 24*(6), 804-808. doi:10.1016/j.ceb.2012.09.007
1417 Henriques, C. M., & Ferreira, M. G. (2024). Telomere length is an epigenetic trait - Implications
1418 for the use of telomerase-deficient organisms to model human disease. *Dis Model*
1419 *Mech, 17*(3). doi:10.1242/dmm.050581
1420 Hernandez-Segura, A., Nehme, J., & Demaria, M. (2018). Hallmarks of Cellular Senescence.
1421 *Trends Cell Biol, 28*(6), 436-453. doi:10.1016/j.tcb.2018.02.001
1422 Hernandez-Silva, D., Canton-Sandoval, J., Martinez-Navarro, F. J., Perez-Sanchez, H., de
1423 Oliveira, S., Mulero, V., . . . Cayuela, M. L. (2022). Senescence-Independent Anti-
1424 Inflammatory Activity of the Senolytic Drugs Dasatinib, Navitoclax, and Venetoclax in
1425 Zebrafish Models of Chronic Inflammation. *Int J Mol Sci, 23*(18).
1426 doi:10.3390/ijms231810468
1427 Huang, W., Hickson, L. J., Eirin, A., Kirkland, J. L., & Lerman, L. O. (2022). Cellular senescence:
1428 the good, the bad and the unknown. *Nat Rev Nephrol, 18*(10), 611-627.
1429 doi:10.1038/s41581-022-00601-z
1430 Hudock, J., & Kenney, J. W. (2024). Aging in zebrafish is associated with reduced locomotor
1431 activity and strain dependent changes in bottom dwelling and thigmotaxis. *PLoS One,*
1432 *19*(5), e0300227. doi:10.1371/journal.pone.0300227
1433 Idda, M. L., McClusky, W. G., Lodde, V., Munk, R., Abdelmohsen, K., Rossi, M., & Gorospe, M.
1434 (2020). Survey of senescent cell markers with age in human tissues. *Aging (Albany NY),*
1435 *12*(5), 4052-4066. doi:10.18632/aging.102903
1436 Idilli, A. I., Cusanelli, E., Pagani, F., Berardinelli, F., Bernabe, M., Cayuela, M. L., . . . Mione, M.
1437 C. (2020). Expression of tert Prevents ALT in Zebrafish Brain Tumors. *Front Cell Dev*
1438 *Biol, 8*, 65. doi:10.3389/fcell.2020.00065
1439 Jaskelioff, M., Muller, F. L., Paik, J.-H., Thomas, E., Jiang, S., Adams, A. C., . . . Depinho, R. a.
1440 (2011). Telomerase reactivation reverses tissue degeneration in aged telomerase-
1441 deficient mice. *Nature, 469*, 102-106. doi:10.1038/nature09603
1442 Jeong, J. Y., Kwon, H. B., Ahn, J. C., Kang, D., Kwon, S. H., Park, J. A., & Kim, K. W. (2008).
1443 Functional and developmental analysis of the blood-brain barrier in zebrafish. *Brain*
1444 *Res Bull, 75*(5), 619-628. doi:10.1016/j.brainresbull.2007.10.043
1445 Jurk, D., Wang, C., Miwa, S., Maddick, M., Korolchuk, V., Tsolou, A., . . . von Zglinicki, T. (2012).
1446 Postmitotic neurons develop a p21-dependent senescence-like phenotype driven by

1447 a DNA damage response. *Aging Cell, 11*(6), 996-1004. doi:10.1111/j.1474-
1448 9726.2012.00870.x
1449 Kacprzak, V., Patel, N. A., Riley, E., Yu, L., Yeh, J. J., & Zhdanova, I. V. (2017). Dopaminergic
1450 control of anxiety in young and aged zebrafish. *Pharmacol Biochem Behav, 157*, 1-8.
1451 doi:10.1016/j.pbb.2017.01.005
1452 Keatinge, M., Bui, H., Menke, A., Chen, Y. C., Sokol, A. M., Bai, Q., . . . Bandmann, O. (2015).
1453 Glucocerebrosidase 1 deficient Danio rerio mirror key pathological aspects of human
1454 Gaucher disease and provide evidence of early microglial activation preceding alpha-
1455 synuclein-independent neuronal cell death. *Hum Mol Genet*.
1456 doi:10.1093/hmg/ddv369
1457 Knox, E. G., Aburto, M. R., Clarke, G., Cryan, J. F., & O'Driscoll, C. M. (2022). The blood-brain
1458 barrier in aging and neurodegeneration. *Mol Psychiatry, 27*(6), 2659-2673.
1459 doi:10.1038/s41380-022-01511-z
1460 Lawson, N. D., Li, R., Shin, M., Grosse, A., Yukselen, O., Stone, O. A., . . . Zhu, L. (2020). An
1461 improved zebrafish transcriptome annotation for sensitive and comprehensive
1462 detection of cell type-specific genes. *eLife, 9*. doi:10.7554/eLife.55792
1463 Lee, H. W., Blasco, M. A., Gottlieb, G. J., Horner, J. W., 2nd, Greider, C. W., & DePinho, R. A.
1464 (1998). Essential role of mouse telomerase in highly proliferative organs. *Nature,*
1465 *392*(6676), 569-574. doi:10.1038/33345
1466 Lee, J., Jo, Y. S., Sung, Y. H., Hwang, I. K., Kim, H., Kim, S. Y., . . . Lee, H. W. (2010). Telomerase
1467 deficiency affects normal brain functions in mice. *Neurochem Res, 35*(2), 211-218.
1468 doi:10.1007/s11064-009-0044-3
1469 Lemoine, M. (2021). The Evolution of the Hallmarks of Aging. *Front Genet, 12*, 693071.
1470 doi:10.3389/fgene.2021.693071
1471 Lex, K., Maia Gil, M., Lopes-Bastos, B., Figueira, M., Marzullo, M., Giannetti, K., . . . Ferreira,
1472 M. G. (2020). Telomere shortening produces an inflammatory environment that
1473 increases tumor incidence in zebrafish. *Proc Natl Acad Sci U S A, 117*(26), 15066-
1474 15074. doi:10.1073/pnas.1920049117
1475 Lopez-Otin, C., Blasco, M. A., Partridge, L., Serrano, M., & Kroemer, G. (2023). Hallmarks of
1476 aging: An expanding universe. *Cell, 186*(2), 243-278. doi:10.1016/j.cell.2022.11.001

1477 Louveau, A., Smirnov, I., Keyes, T. J., Eccles, J. D., Rouhani, S. J., Peske, J. D., . . . Kipnis, J.
1478 (2015). Structural and functional features of central nervous system lymphatic vessels.
1479 *Nature, 523*(7560), 337-341. doi:10.1038/nature14432
1480 Lujambio, A. (2016). To clear, or not to clear (senescent cells)? That is the question. *Bioessays,*
1481 *38 Suppl 1*, S56-64. doi:10.1002/bies.201670910
1482 M, I. F. A. F. C., Selman;, H. A. M. A. L.-C. C., Lene, E. F. E. S. G. J. L. T. J. M., & Bellantuono, J.
1483 R. S. X. T. E. I. (2016). Interventions for age-related diseases: shifting the paradigm.
1484 *Mech Ageing Dev*(in press).
1485 Martin-Ruiz, C., Williams-Gray, C. H., Yarnall, A. J., Boucher, J. J., Lawson, R. A., Wijeyekoon,
1486 R. S., . . . Saretzki, G. (2020). Senescence and Inflammatory Markers for Predicting
1487 Clinical Progression in Parkinson's Disease: The ICICLE-PD Study. *J Parkinsons Dis,*
1488 *10*(1), 193-206. doi:10.3233/JPD-191724
1489 Martins, R. R., Ellis, P. S., MacDonald, R. B., Richardson, R. J., & Henriques, C. M. (2019).
1490 Resident Immunity in Tissue Repair and Maintenance: The Zebrafish Model Coming of
1491 Age. *Front Cell Dev Biol, 7*, 12. doi:10.3389/fcell.2019.00012
1492 Mathias, J. R., Dodd, M. E., Walters, K. B., Yoo, S. K., Erik, A., & Huttenlocher, A. (2010).
1493 Characterization of Zebrafish Larval Inflammatory Macrophages Jonathan.
1494 *Developmental and comparative immunology, 33*, 1212-1217.
1495 doi:10.1016/j.dci.2009.07.003.Characterization
1496 Mattiussi, M., Tilman, G., Lenglez, S., & Decottignies, A. (2012). Human telomerase represses
1497 ROS-dependent cellular responses to Tumor Necrosis Factor-α without affecting NF-
1498 κB activation. *Cellular signalling, 24*, 708-717. doi:10.1016/j.cellsig.2011.11.004
1499 Maximino, C., de Brito, T. M., da Silva Batista, A. W., Herculano, A. M., Morato, S., & Gouveia,
1500 A., Jr. (2010). Measuring anxiety in zebrafish: a critical review. *Behav Brain Res, 214*(2),
1501 157-171. doi:10.1016/j.bbr.2010.05.031
1502 Meeker, R. B., Williams, K., Killebrew, D. A., & Hudson, L. C. (2012). Cell trafficking through
1503 the choroid plexus. *Cell Adh Migr, 6*(5), 390-396. doi:10.4161/cam.21054
1504 Muldoon, L. L., Alvarez, J. I., Begley, D. J., Boado, R. J., Del Zoppo, G. J., Doolittle, N. D., . . .
1505 Neuwelt, E. A. (2013). Immunologic privilege in the central nervous system and the
1506 blood-brain barrier. *J Cereb Blood Flow Metab, 33*(1), 13-21.
1507 doi:10.1038/jcbfm.2012.153

1508 Nolte, E. D., Nolte, K. A., & Yan, S. S. (2019). Anxiety and task performance changes in an aging
1509 mouse model. *Biochem Biophys Res Commun, 514*(1), 246-251.
1510 doi:10.1016/j.bbrc.2019.04.049
1511 Oosterhof, N., Holtman, I. R., Kuil, L. E., van der Linde, H. C., Boddeke, E. W., Eggen, B. J., &
1512 van Ham, T. J. (2017). Identification of a conserved and acute neurodegeneration-
1513 specific microglial transcriptome in the zebrafish. *Glia, 65*(1), 138-149.
1514 doi:10.1002/glia.23083
1515 Ovadya, Y., & Krizhanovsky, V. (2014). Senescent cells: SASPected drivers of age-related
1516 pathologies. *Biogerontology, 15*, 627-642. doi:10.1007/s10522-014-9529-9
1517 Pakulski, C., Drobnik, L., & Millo, B. (2000). Age and sex as factors modifying the function of
1518 the blood-cerebrospinal fluid barrier. *Med Sci Monit, 6*(2), 314-318.
1519 Panca, M., Livingston, G., Barber, J., Cooper, C., La Frenais, F., Marston, L., . . . Hunter, R. M.
1520 (2019). Healthcare resource utilisation and costs of agitation in people with dementia
1521 living in care homes in England - The Managing Agitation and Raising QUality of LifE in
1522 Dementia (MARQUE) study. *PLoS One, 14*(2), e0211953.
1523 doi:10.1371/journal.pone.0211953
1524 Papageorgakopoulou, M. A., Bania, A., Lagogianni, I. A., Birmpas, K., & Assimakopoulou, M.
1525 (2024). The Role of Glia Telomere Dysfunction in the Pathogenesis of Central Nervous
1526 System Diseases. *Mol Neurobiol, 61*(8), 5868-5881. doi:10.1007/s12035-024-03947-6
1527 Pegram, R. G., Smith, R., Franklin, R., Gallagher, T., Oosterwijk, G., & Wilsmore, A. J. (1991).
1528 Comparison of the calf suckling technique and milk oxytocin test for estimation of milk
1529 yields. *Trop Anim Health Prod, 23*(2), 99-102. doi:10.1007/BF02361190
1530 Pereira, B. I., Devine, O. P., Vukmanovic-Stejic, M., Chambers, E. S., Subramanian, P., Patel,
1531 N., . . . Akbar, A. N. (2019). Senescent cells evade immune clearance via HLA-E-
1532 mediated NK and CD8(+) T cell inhibition. *Nat Commun, 10*(1), 2387.
1533 doi:10.1038/s41467-019-10335-5
1534 Petrova, N. V., Velichko, A. K., Razin, S. V., & Kantidze, O. L. (2016). Small molecule compounds
1535 that induce cellular senescence. *Aging Cell, 15*(6), 999-1017. doi:10.1111/acel.12518
1536 Rahman, R., Latonen, L., & Wiman, K. G. (2005). hTERT antagonizes p53-induced apoptosis
1537 independently of telomerase activity. *Oncogene, 24*(8), 1320-1327.
1538 doi:10.1038/sj.onc.1208232

Raj, D. D. A., Moser, J., van der Pol, S. M. A., van Os, R. P., Holtman, I. R., Brouwer, N., . . . Boddeke, H. W. G. M. (2015). Enhanced microglial pro-inflammatory response to lipopolysaccharide correlates with brain infiltration and blood-brain barrier dysregulation in a mouse model of telomere shortening. *Aging Cell*, 1003-1013. doi:10.1111/acel.12370

Ramanathan, R., Kohli, A., Ingaramo, M. C., Jain, A., Leng, S. X., Punjabi, N. M., . . . Fedarko, N. S. (2013). Serum chitotriosidase, a putative marker of chronically activated macrophages, increases with normal aging. *J Gerontol A Biol Sci Med Sci, 68*(10), 1303-1309. doi:10.1093/gerona/glt022

Recagni, M., Bidzinska, J., Zaffaroni, N., & Folini, M. (2020). The Role of Alternative Lengthening of Telomeres Mechanism in Cancer: Translational and Therapeutic Implications. *Cancers (Basel), 12*(4). doi:10.3390/cancers12040949

Redd, M. J., Kelly, G., Dunn, G., Way, M., & Martin, P. (2006). Imaging macrophage chemotaxis in vivo: studies of microtubule function in zebrafish wound inflammation. *Cell motility and the cytoskeleton, 63*, 415-422. doi:10.1002/cm.20133

Righi, D., Manco, C., Pardini, M., Stufano, A., Schino, V., Pelagotti, V., . . . Plantone, D. (2024). Investigating interleukin-8 in Alzheimer's disease: A comprehensive review. *J Alzheimers Dis*, 13872877241298973. doi:10.1177/13872877241298973

Romaniuk, A., Paszel-Jaworska, A., Toton, E., Lisiak, N., Holysz, H., Krolak, A., . . . Rubis, B. (2018). The non-canonical functions of telomerase: to turn off or not to turn off. *Mol Biol Rep*. doi:10.1007/s11033-018-4496-x

Rossiello, F., Herbig, U., Longhese, M. P., Fumagalli, M., & d'Adda di Fagagna, F. (2014). Irreparable telomeric DNA damage and persistent DDR signalling as a shared causative mechanism of cellular senescence and ageing. *Curr Opin Genet Dev, 26*, 89-95. doi:10.1016/j.gde.2014.06.009

Samant, R. R., Standaert, D. G., & Harms, A. S. (2024). The emerging role of disease-associated microglia in Parkinson's disease. *Front Cell Neurosci, 18*, 1476461. doi:10.3389/fncel.2024.1476461

Sarin, K. Y., Cheung, P., Gilison, D., Lee, E., Tennen, R. I., Wang, E., . . . Artandi, S. E. (2005). Conditional telomerase induction causes proliferation of hair follicle stem cells. *Nature, 436*(7053), 1048-1052. doi:10.1038/nature03836

1570 Schaum, N., Lehallier, B., Hahn, O., Palovics, R., Hosseinzadeh, S., Lee, S. E., . . . Wyss-Coray,
1571 T. (2020). Ageing hallmarks exhibit organ-specific temporal signatures. *Nature,*
1572 *583*(7817), 596-602. doi:10.1038/s41586-020-2499-y
1573 Segal-Bendirdjian, E., & Geli, V. (2019). Non-canonical Roles of Telomerase: Unraveling the
1574 Imbroglio. *Front Cell Dev Biol, 7*, 332. doi:10.3389/fcell.2019.00332
1575 Spilsbury, A., Miwa, S., Attems, J., & Saretzki, G. (2015). The role of telomerase protein TERT
1576 in Alzheimer's disease and in tau-related pathology in vitro. *Journal of Neuroscience,*
1577 *35*(4), 1659-1674. doi:10.1523/JNEUROSCI.2925-14.2015
1578 Sprungala, S. (2009). Telomere length, telomerase and maintenance of stem cells in
1579 the adult zebrafish brain. In. TECHNISCHE UNIVERSITÄT MÜNCHEN.
1580 Steinacker, P., Verde, F., Fang, L., Feneberg, E., Oeckl, P., Roeber, S., . . . group, F. T. s. (2018).
1581 Chitotriosidase (CHIT1) is increased in microglia and macrophages in spinal cord of
1582 amyotrophic lateral sclerosis and cerebrospinal fluid levels correlate with disease
1583 severity and progression. *J Neurol Neurosurg Psychiatry, 89*(3), 239-247.
1584 doi:10.1136/jnnp-2017-317138
1585 Strominger, I., Elyahu, Y., Berner, O., Reckhow, J., Mittal, K., Nemirovsky, A., & Monsonego,
1586 A. (2018). The Choroid Plexus Functions as a Niche for T-Cell Stimulation Within the
1587 Central Nervous System. *Front Immunol, 9*, 1066. doi:10.3389/fimmu.2018.01066
1588 Sullivan, D. I., Jiang, M., Hinchie, A. M., Roth, M. G., Bahudhanapati, H., Nouraie, M., . . . Alder,
1589 J. K. (2021). Transcriptional and Proteomic Characterization of Telomere-Induced
1590 Senescence in a Human Alveolar Epithelial Cell Line. *Front Med (Lausanne), 8*, 600626.
1591 doi:10.3389/fmed.2021.600626
1592 Sung, Y. H., Ali, M., & Lee, H. W. (2014). Extracting extra-telomeric phenotypes from
1593 telomerase mouse models. *Yonsei Medical Journal, 55*, 1-8.
1594 doi:10.3349/ymj.2014.55.1.1
1595 Sweeney, M. D., Zhao, Z., Montagne, A., Nelson, A. R., & Zlokovic, B. V. (2019). Blood-Brain
1596 Barrier: From Physiology to Disease and Back. *Physiol Rev, 99*(1), 21-78.
1597 doi:10.1152/physrev.00050.2017
1598 Tabula Muris, C. (2020). A single-cell transcriptomic atlas characterizes ageing tissues in the
1599 mouse. *Nature, 583*(7817), 590-595. doi:10.1038/s41586-020-2496-1

1600 Tarr, A. J., Chen, Q., Wang, Y., Sheridan, J. F., & Quan, N. (2012). Neural and behavioral
1601 responses to low-grade inflammation. *Behav Brain Res, 235*(2), 334-341.
1602 doi:10.1016/j.bbr.2012.07.038
1603 Topiwala, A., Nichols, T. E., Williams, L. Z. J., Robinson, E. C., Alfaro-Almagro, F., Taschler, B., .
1604 . . Smith, S. M. (2023). Telomere length and brain imaging phenotypes in UK Biobank.
1605 *PLoS One, 18*(3), e0282363. doi:10.1371/journal.pone.0282363
1606 Tripathi, U., Misra, A., Tchkonia, T., & Kirkland, J. L. (2021). Impact of Senescent Cell Subtypes
1607 on Tissue Dysfunction and Repair: Importance and Research Questions. *Mech Ageing*
1608 *Dev, 198*, 111548. doi:10.1016/j.mad.2021.111548
1609 Tuttle, C. S. L., Luesken, S. W. M., Waaijer, M. E. C., & Maier, A. B. (2021). Senescence in tissue
1610 samples of humans with age-related diseases: A systematic review. *Ageing Res Rev,*
1611 *68*, 101334. doi:10.1016/j.arr.2021.101334
1612 Van Houcke, J., Bollaerts, I., Geeraerts, E., Davis, B., Beckers, A., Van Hove, I., . . . Moons, L.
1613 (2017). Successful optic nerve regeneration in the senescent zebrafish despite age-
1614 related decline of cell intrinsic and extrinsic response processes. *Neurobiol Aging, 60*,
1615 1-10. doi:10.1016/j.neurobiolaging.2017.08.013
1616 Vasconcelos, R. O., Gordillo-Martinez, F., Ramos, A., & Lau, I. H. (2023). Effects of Noise
1617 Exposure and Ageing on Anxiety and Social Behaviour in Zebrafish. *Biology (Basel),*
1618 *12*(9). doi:10.3390/biology12091165
1619 Vazquez-Villasenor, I., Garwood, C. J., Heath, P. R., Simpson, J. E., Ince, P. G., & Wharton, S. B.
1620 (2020). Expression of p16 and p21 in the frontal association cortex of ALS/MND brains
1621 suggests neuronal cell cycle dysregulation and astrocyte senescence in early stages of
1622 the disease. *Neuropathol Appl Neurobiol, 46*(2), 171-185. doi:10.1111/nan.12559
1623 Vellingiri, B., Balasubramani, K., Iyer, M., Raj, N., Elangovan, A., Song, K., . . . Cho, S. G. (2023).
1624 Role of Telomeres and Telomerase in Parkinson's Disease-A New Theranostics? *Adv*
1625 *Biol (Weinh), 7*(12), e2300097. doi:10.1002/adbi.202300097
1626 Wang, Y., Kuca, K., You, L., Nepovimova, E., Heger, Z., Valko, M., . . . Jomova, K. (2024). The
1627 role of cellular senescence in neurodegenerative diseases. *Arch Toxicol, 98*(8), 2393-
1628 2408. doi:10.1007/s00204-024-03768-5
1629 Wittenberg, R., Knapp, M., Hu, B., Comas-Herrera, A., King, D., Rehill, A., . . . Kingston, A.
1630 (2019). The costs of dementia in England. *Int J Geriatr Psychiatry, 34*(7), 1095-1103.
1631 doi:10.1002/gps.5113

1632 Wright, D., Nakamichi, R., Krause, J., & Butlin, R. K. (2006). QTL analysis of behavioral and
1633 morphological differentiation between wild and laboratory zebrafish (Danio rerio).
1634 *Behav Genet, 36*(2), 271-284. doi:10.1007/s10519-005-9029-4
1635 Xu, M., Tchkonia, T., Ding, H., Ogrodnik, M., Lubbers, E. R., Pirtskhalava, T., . . . Kirkland, J. L.
1636 (2015). JAK inhibition alleviates the cellular senescence-associated secretory
1637 phenotype and frailty in old age. *Proc Natl Acad Sci U S A, 112*(46), E6301-6310.
1638 doi:10.1073/pnas.1515386112
1639 Yu, X., Liu, M. M., Zheng, C. Y., Liu, Y. T., Wang, Z., & Wang, Z. Y. (2023). Telomerase reverse
1640 transcriptase and neurodegenerative diseases. *Front Immunol, 14*, 1165632.
1641 doi:10.3389/fimmu.2023.1165632
1642 Zambusi, A., Pelin Burhan, O., Di Giaimo, R., Schmid, B., & Ninkovic, J. (2020). Granulins
1643 Regulate Aging Kinetics in the Adult Zebrafish Telencephalon. *Cells, 9*(2).
1644 doi:10.3390/cells9020350
1645 Zane, F., Bouzid, H., Sosa Marmol, S., Brazane, M., Besse, S., Molina, J. L., . . . Rera, M. (2023).
1646 Smurfness-based two-phase model of ageing helps deconvolve the ageing
1647 transcriptional signature. *Aging Cell, 22*(11), e13946. doi:10.1111/acel.13946
1648 Zhang, M. J., Pisco, A. O., Darmanis, S., & Zou, J. (2021). Mouse aging cell atlas analysis reveals
1649 global and cell type-specific aging signatures. *eLife, 10*. doi:10.7554/eLife.62293
1650